Article

The Polyhomologation of 1-Boraadamantane: Mapping the Migration Pathways of a Propagating Macrotricyclic Trialkylborane

Carl E. Wagner, Jang-Seob Kim, and Kenneth J. Shea

J. Am. Chem. Soc., **2003**, 125 (40), 12179-12195• DOI: 10.1021/ja0361291 • Publication Date (Web): 17 September 2003

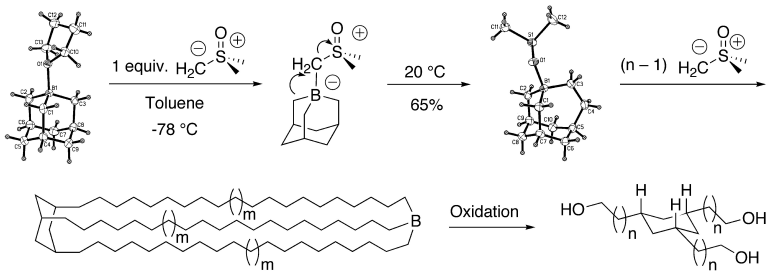

More About This Article

Additional resources and features associated with this article are available within the HTML version:

- Supporting Information
- Links to the 4 articles that cite this article, as of the time of this article download
- Access to high resolution figures
- Links to articles and content related to this article
- Copyright permission to reproduce figures and/or text from this article

View the Full Text HTML

J|A|C|S
ARTICLES
Published on Web 09/17/2003

The Polyhomologation of 1-Boraadamantane: Mapping the Migration Pathways of a Propagating Macrotricyclic Trialkylborane

Carl E. Wagner,[†] Jang-Seob Kim,[‡] and Kenneth J. Shea*,[†]

Contribution from the Department of Chemistry, University of California Irvine, Irvine, California 92697, and Department of Chemistry, Daegu University, Gyungsan, Gyunbuk 712-714, South Korea

Received May 14, 2003; E-mail: kjshea@uci.edu

Abstract: Trialkyl and triaryl organoboranes undergo multiple, repetitive homologations upon reaction with dimethylsulfoxonium methylide (**1**). This multiple homologation reaction, or polyhomologation, produces polymethylene in a living reaction. Applying the polyhomologation reaction to cyclic and polycyclic organoboranes permits the construction of unique oligomeric and polymeric architectures that are not readily accessible by standard olefin polymerization. The polyhomologation of 1-boraadamantane·THF (**2**) by ylide **1** generates novel macrotricyclic trialkylboranes (**3**). The oxidation of these macrocyclic organoboranes generates a three-armed star polymethylene polymer (**4**) incorporating a *cis,cis*-1,3,5-trisubstituted cyclohexane core. Interestingly, only one-third of the initiators lead to product formation, resulting in an observed degree of polymerization 3 times higher than expected. Close examination of the initial stages of polymerization show that 1-boraadamantane·THF reacts with 1 equiv of **1** to afford a monohomologated product. Subsequent homologations were found to contain branch points leading to isomeric tricyclic products after the third, fourth, and fifth methylene insertions. At these stages of homologation, all of the propagating species result in tricyclic trialkylborane cages with collapsed, inverted pyramidal boron centers that are substantially less reactive toward ylide. Approximately two-thirds of the species discontinue polymerization at these stages. However, one-third of these species continue to propagate and eventually result in the formation of giant macrotricyclic polymers of narrow polydispersity. Molecular modeling and kinetic simulation have aided in the analysis of the probable pathways through which the reaction proceeds.

Introduction

Hydrocarbon polymers constitute one of the world's leading sources of synthetically derived materials.[1] An increasing demand for high-performance polymers has necessitated the development of new catalysts, monomers, and polymerization techniques that permit greater control over factors that influence the physical properties of the polymers.[2] Despite advances in the development of efficient catalysts, there are still many synthetic challenges remaining to be solved. Studies in our laboratory have concentrated on developing a new living polymethylene synthesis based on the polymerization of dimethylsulfoxonium methylide (**1**) by trialkylboranes. In this reaction, the alkyl groups of the trialkylboranes undergo repetitive 1,2-migrations with ylide monomers to build the carbon backbone of the developing polymethylene polymers one carbon at a time. This process of repetitive 1,2-migration, or homologation, has been termed polyhomologation.[3] Indeed, the polyhomologation reaction has demonstrated its versatility in the construction of novel materials ranging from copolymers of polymethylene and poly(dimethylsiloxane)s[4] to the commercially important commodity copolymer poly(ethylene-*b*-styrene).[5] By developing and combining new monomer sources, the polyhomologation reaction has also yielded a route to a material with the same chemical composition as an ethylene-propylene copolymer.[6]

Additionally, the polyhomologation of cyclic and bicyclic organoboranes has demonstrated routes to oligomeric and polymeric boracyclanes and carbocyclics.[7] Applying the polyhomologation reaction to polycyclic organoboranes offers an opportunity for the construction of novel topologies such as

[†] University of California Irvine.
[‡] Daegu University.

(1) (a) Barghoorn, P.; Stebani, U.; Balsam, M. *Adv. Mater*. **1998**, *10*, 635. (b) Morse, P. M. *Chem. Eng. News* **1999**, *77*, 11. (c) Younkin, T. R.; Connor, E. F.; Henderson, J. I.; Friedrich, S. K.; Grubbs, R. H.; Bansleben, D. A. *Science* **2000**, *287*, 460. (d) Wilson, E. *Chem. Eng. News* **2000**, *78*, 14.

(2) (a) Brintzinger, H. H.; Fisher, D.; Müelhaupt, R.; Rieger, B.; Waymouth, R. M. *Angew. Chem., Int. Ed. Engl.* **1995**, *34*, 1143. (b) Fink, G., Müelhaupt, R., Brintzinger, H. H., Eds. *ts: Recent Scientific Innovations and Technological Improvement*; Springer-Verlag: Berlin, 1995. (c) Coates, G. W.; Waymouth, R. M. *Comprehensive Organometallic Chemistry II*; Pergamon Press: Elmsford, NY, 1995; Vol. 12, p 1193. (d) Britovsek, G. J. P.; Givson, V. C.; Wass, D. F. *Angew. Chem., Int. Ed.* **1999**, *38*, 428. (e) Coates, G. W. *Chem. Rev.* **2000**, *100*, 1223. (f) Ittel, S. D.; Johnson, L. K.; Brookhart, M. *Chem. Rev.* **2000**, *100*, 1169. (g)Mark, T. J.; Chen, E. Y. *Chem. Rev.* **2000**, *100*, 1391. (h) Matyjaszeweski, K.; Xia, J. *Chem. Rev.* **2001**, *101*, 2921.

(3) Shea, K. J.; Walker, J. W.; Zhu, H.; Paz, M.; Greaves, J. *J. Am. Chem. Soc.* **1997**, *119*, 9049.

(4) Shea, K. J.; Staiger, C. L.; Lee, S. Y. *Macromolecules* **1999**, *32*, 3157.

(5) Zhou, X.-Z.; Shea, K. J. *Macromolecules* **2001**, *34*, 3114.

(6) Zhou, X.-Z.; Shea, K. J. *J. Am. Chem. Soc.* **2000**, *122*, 11515.

(7) (a) Shea, K. J.; Lee, S. Y.; Busch, B. B. *J. Org. Chem.* **1998**, *63*, 5746. (b) Shea, K. J.; Busch, B. B.; Paz, M. *Angew. Chem., Int. Ed.* **1998**, *37*, 1391.

Scheme 1

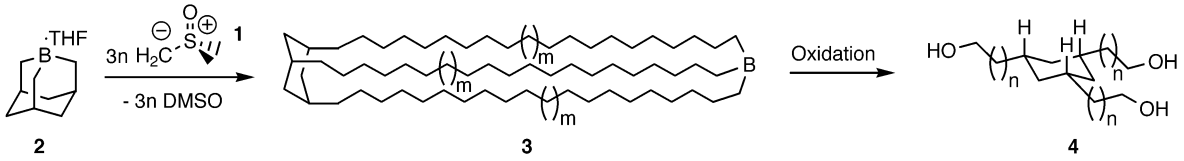

Scheme 2

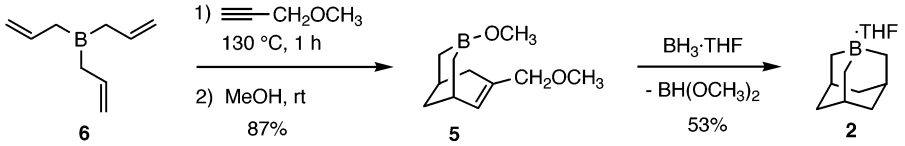

macrotricyclic organoboranes capped with a Lewis acid center. These structures may be elaborated to hydrocarbon star polymer architectures.[8] 1-Boraadamantane·THF (**2**)[9] was selected for study as a tricyclic alkylborane initiator to access a three-armed star polymethylene polymer, with the arms radiating from a cyclohexane core. In this strategy, trialkylborane **2** would serve as an initiator, while dimethylsulfoxonium methylide (**1**) would serve as a methylene monomer source. One equivalent of DMSO would be expelled for each equivalent of ylide **1** consumed. Random insertion into all three carbon−boron bonds would result in the formation of a hyperextended macrotricyclic organoborane (**3**). The living nature of the polyhomologation reaction would allow control of the length of each wall of **3**.[10] Providing each branch grows randomly, subsequent oxidation of **3** would provide a regular star polymer **4** (Scheme 1).

The strategy thus outlined was undertaken, and the results are discussed below.

Results and Discussion

Thus, 1-boraadamantane·THF (**2**) was synthesized by the hydroboration of 3-methoxy-7-(methoxymethyl)-3-borabicyclo-[3.3.1]non-6-ene (**5**). This compound was prepared by the reaction of triallylborane (**6**) with methyl propargyl ether followed by methanolysis, according to the procedure of Mikhailov and co-workers (Scheme 2).[11] Triallylborane (**6**) was synthesized according to the method of Zakharkin and co-workers.[12]

Complex **2**, a white crystalline solid that slowly degrades in air, was purified by vacuum sublimation, and its structure was confirmed by X-ray crystallography (Figure 1).

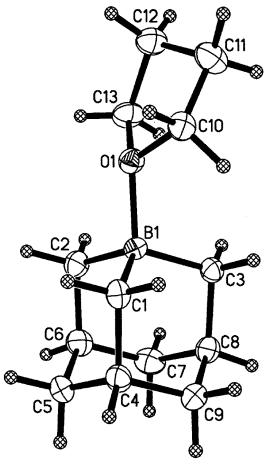

Figure 1. The X-ray crystal structure of 1-boraadamantane·THF (**2**).

Free 1-boraadamantane has been reported by Mikhailov and co-workers to be highly reactive and predisposed to complex formation with Lewis bases.[13] However, an apparent glass transition occurring at 183 K renders solid 1-boraadamantane amorphous at room temperature.[14] The geometry optimized structure of free 1-boraadamantane at the RB3LYP/6-311**G level of theory shows a B−C bond distance of 1.569 Å and ∠CBC = 116.4°.[15] These values are in accord with the values of 1.574 Å and 116.3° calculated at the HF/3-21G* level of theory used throughout this study. The $\theta_{\sigma\pi}$ parameter of the POAV1 analysis measures the angle between a π-bond orbital and the σ-orbitals for a distorted sp^2 atom in an aromatic system.[16] This parameter was modified to measure the angle ($\theta_{\sigma p}$) between the empty p-orbital on boron and the σ orbitals to the carbon atoms to assess the degree of pyramidalization for free 1-boraadamantane. The value of $\theta_{\sigma p} - 90°$ is a convenient expression of this parameter, and it ranges from 0° for a trigonal planar sp^2 atom to 19.5° for a tetrahedral sp^3 atom.[17] The $\theta_{\sigma p} - 90°$ value for the HF/3-21G* geometry optimized structure of free 1-boraadamantane is 11.1°, corresponding to a 57% pyramidalization. The geometrically imposed prehybridization about the boron center of free 1-boraadamantane likely predisposes 1-boraadamantane to readily form tetrahedral complexes with Lewis basic substrates. Indeed, 1-boraadamantane displays a remarkable capacity to form stable complexes with Lewis basic substrates such as pyridine[18] as well as weakly Lewis basic substrates such as ether and THF. The X-ray diffraction study shows that complex **2** adopts a tetrahedral geometry with B−O = 1.64 Å, B−C = 1.61 Å, $\angle O_1B_1C_1 = \angle O_1B_1C_2 = 107°$, and $\angle O_1B_1C_3 = 111°$.

(8) Wagner, C. E.; Shea, K. J. *Org. Lett.* **2001**, *3*, 3063.
(9) (a) Mikhailov, B. M. *Pure Appl. Chem.* **1980**, *52*, 691. (b) Mikhailov, B. M. *Izv. Akad. Nauk SSSR, Ser. Khim.* **1984**, *33*, 225.
(10) Shea, K. J. *Chem.-Eur. J.* **2000**, *6*, 1113.
(11) (a) Mikhailov, B. M.; Baryshnikova, T. K.; Kiselev, V. G.; Shashkov, A. S. *Izv. Akad. Nauk SSSR, Ser. Khim.* **1979**, *28*, 2544. (b) Mikhailov, B. M.; Baryshnikova, T. K. *Izv. Akad. Nauk SSSR, Ser. Khim.* **1979**, *28*, 2541.
(12) Zakharkin, L. I.; Stanko, V. I. *Izv. Akad. Nauk SSSR, Otd. Khim. Nauk* **1960**, 1896.
(13) (a) Mikhailov, B. M.; Smirnov, V. N. *Izv. Akad. Nauk SSSR, Ser. Khim.* **1973**, *22*, 2165. (b) Mikhailov, B. M.; Smirnov, V. N. *Izv. Akad. Nauk SSSR, Ser. Khim.* **1974**, *23*, 1137. (c) Mikhailov, B. M.; Smirnov, V. N.; Kasparov, V. A. *Izv. Akad. Nauk SSSR, Ser. Khim.* **1976**, *25*, 2302.
(14) Bukalov, S. S.; Leites, L. A.; Bubnov, Yu. N.; Gurskii, M. E.; Potapova, T. V. *Izv. Akad. Nauk SSSR, Ser. Khim.* **1989**, *38*, 483.
(15) Wrackmeyer, B.; Wolfgang, M.; Tok, O. L.; Bubnov, Y. N. *Chem.-Eur. J.* **2002**, *8*, 1537.
(16) (a) Haddon, R. C.; Scott, L. T. *Pure Appl. Chem.* **1986**, *58*, 137. (b) Haddon, R. C. *J. Am. Chem. Soc.* **1986**, *108*, 2837.
(17) Haddon, R. C. *J. Am. Chem. Soc.* **1990**, *112*, 3385.
(18) Vorontsova, L. G.; Chizhov, O. S.; Smirnov, V. N.; Mikhailov, B. M. *Izv. Akad. Nauk SSSR, Ser. Khim.* **1981**, *30*, 595.

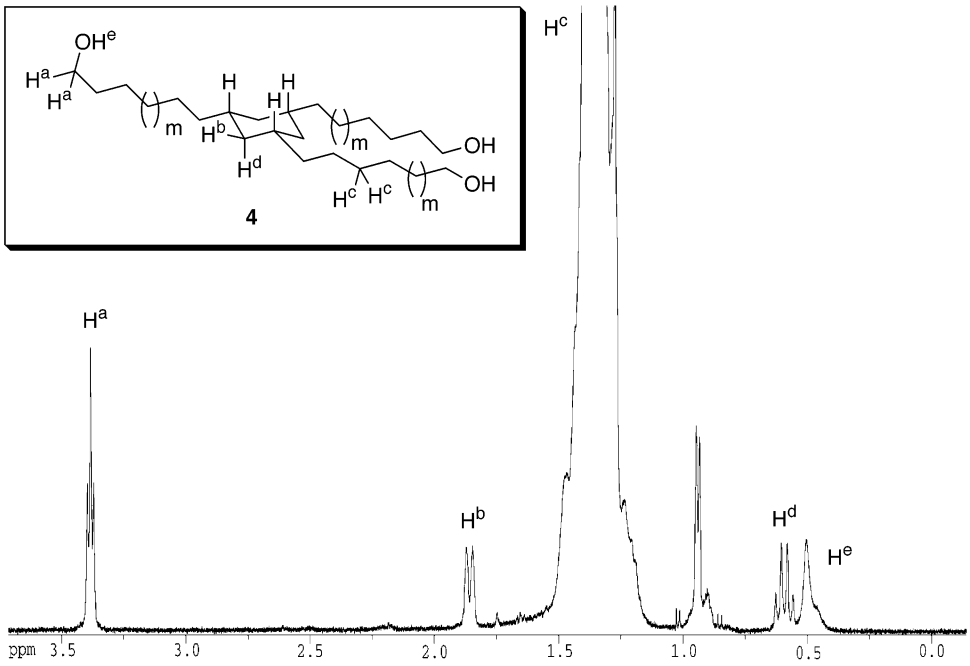

Figure 2. Representative ^{1}H NMR spectrum of polymeric triol **4** (C_6D_6, 78 °C, 500 MHz). This spectrum is that of the polymeric product of trial 2 in Table 1. The doublet at 0.9 ppm arises from the incorporation of 1−2% ethylidene groups in the polymethylene backbone arising from dimethylsulfoxonium ethylide, formed as a minor product in the synthesis of ylide **1**.[21] The broad singlet at 0.5 ppm has been assigned to the hydroxy-protons of the end groups.

Scheme 3

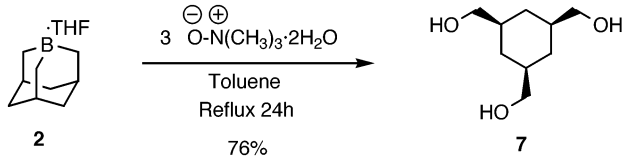

The homologation reaction involves a two-step process consisting of addition of the nucleophilic ylide **1** to form an "ate" complex followed by a [1,2]-migration. Related migrations of bicyclic organoboranes proceed via an antiperiplanar transition state.[19] To establish the compatibility of the 1-boraadamantane core with addition-migration, we first examined its oxidation. Compound **2** is readily oxidized by trimethylamine *N*-oxide dihydrate[20] (TAO), to give the triol, *cis*,*cis*-1,3,5-tris-(hydroxymethyl)cyclohexane (**7**), in 76% yield (Scheme 3).

1-Boraadamantane·THF (**2**) was next examined as an initiator for the polyhomologation reaction. Toluene solutions of ylide **1** were preheated to 80 °C and treated with an aliquot of a toluene solution of **2**. The ylide was rapidly consumed (5 min). TAO was added directly to the solution to effect oxidation under reflux conditions. Removal of solvents followed by filtering and washing of the polymeric solids with methanol, water, and hexanes gave near quantitative crude yields of polymeric triol **4**. Samples were further purified by reprecipitation in toluene/acetonitrile to afford an opaque white polymer in 88−94% yield. The structural assignment of the star polymeric triols **4** is as follows.

The ^{1}H NMR spectra of the polymer **4** (C_6D_6, 78 °C) produced by these reactions have features consistent with a regular star architecture. The spectra include a triplet at 3.38 ppm (J = 6.4 Hz) corresponding to the terminal hydroxymethylene protons of **4**. Also, there is an apparent doublet at 1.85 ppm (J = 12.2 Hz) and a quartet at 0.59 ppm (J = 11.8 Hz) corresponding to the equatorial and axial methylene protons of the cyclohexane ring of **4** (Figure 2).

Table 1. Molecular Weight Data for Star Polymers **4**

trial	DP[a] (calcd)	M_N[b] (g/mol)	DP[b]	DP[c] ^{1}H NMR	dead catalysts (%)[c] ^{1}H NMR	PDI[b]
1	25	2403	53	73	66	1.06
2	50	5595	129	148	66	1.09
3	69	10 542	246	190	63	1.08
4	138	19 613	462	345	60	1.08

[a] The DP refers to n (Scheme 1). [b] Data refer to GPC in *o*-xylenes at 100 °C calibrated with linear polyethylene standards. [c] Data refer to ^{1}H NMR end group analysis (i.e., the ratio of the terminal hydroxymethylene protons to the broad polymethylene peak of **4**).

Lightly branched polymers of the type of **4** comprised of unsymmetrical branches (i.e., two long branches and one short branch) would not be expected to exhibit apparent three-fold symmetry of the axial and equatorial hydrogens of the cyclohexane core. The clear three-fold pseudosymmetry of the equatorial and axial protons, as well as the multiplicity of the terminal hydroxymethylene groups of **4**, support the conclusion that all three branches of the propagating species participate in migration.

The degree of polymerization (DP) was established by GPC and ^{1}H NMR end group analysis (Table 1). Reactions were run with initial ratios of (1/3)ylide:boraadamantane of 25, 50, 69, and 138. These reactions should produce regular star polymers **4** with n = 25, 50, 69, and 138, respectively (Scheme 1). In all cases, however, the DP by ^{1}H NMR end group analysis was consistently 3 times greater than the calculated DP.

While the GPC was calibrated with linear polyethylene standards, corrections for star topology should result in observed (GPC) molecular weights that are lower than the calculated molecular weight on the basis of stoichiometry.[22] Furthermore, previous examples of regular three-armed star polymethylene

(19) Soderquist, J. A.; Najafi, M. R. *J. Org. Chem.* **1986**, *51*, 1330.
(20) Kabalka, G. W.; Hedgecock, H. C., Jr. *J. Org. Chem.* **1975**, *40*, 1776.

carbinol polymers resulted in polymers whose theoretical and observed molecular weights by GPC corresponded within 10%.[10] Importantly, the PDIs of all trials in the present study are <1.09. Such narrow PDIs are characteristic of living polymerization.

Additionally, two reactions were conducted to give star polymers **4** in the molecular weight range appropriate to characterize the nature of the chain branching. The difference between polymers exhibiting long chain branching and linear chain polymers is frequently expressed according to the Zimm—Stockmayer model[23] in terms of the square of the radius of gyration of a branched polymer as compared to that of a linear polymer of the same molecular weight. This ratio, g, is given below.

$$g = \frac{\langle R_g^2 \rangle_{\text{branched}}}{\langle R_g^2 \rangle_{\text{linear}}}$$

For a three-armed A_2B star polymer, the Zimm—Stockmayer model[23] gives the following predicted value for g.

$$g^{\text{pred}} = 1 - \frac{6s}{(s+2)^3}$$

where $s = M_A/M_B$ is the ratio of the A arm molecular weight (M_A) to the B arm molecular weight (M_B). For a regular star polymer, $M_A = M_B$, and $g^{\text{pred}} = 0.778$.

Another common characterization of long chain branching in star polymers arises from the comparison of the intrinsic viscosity (η) of a given star polymer to the viscosity of a linear polymer of the same molecular weight.[24] This ratio, g', is given below.

$$g' = \frac{[\eta]_{\text{branched}}}{[\eta]_{\text{linear}}}$$

The relation between g' and g is expressed in an equation with the exponent, ϵ, as shown below.

$$g' = g^{\epsilon}$$

For a three-armed regular star polymer, g' can be approximated as the square root of g,[25] although experimentally it has been found that $\epsilon \approx 0.6$ for stars and other branched comb polymers.[26]

The technique of triple detector GPC involves a combination of GPC, light scattering, and viscometry. Triple detector GPC according to the method of deGroot and co-workers[27] was applied to the high molecular weight star polymers **4** to determine absolute molecular weights by light scattering and intrinsic viscosity by viscometry. The data for the star polymers **4**, including the experimental values of g' and g, are summarized in Table 2.

Table 2. Light Scattering, Viscosity, and GPC Data for High Molecular Weight Star Polymers **4**

trial	DP[a] (calcd)	M_w[b] (g/mol)	DP[b]	$[\eta]$[c] (dL/g)	g'[c]	g[d] ($\epsilon = 0.5$)	PDI[e]
1	296	24 270	573	0.567	0.887	0.787	1.12
2	593	39 650	938	0.805	0.878	0.771	1.12

[a] The DP refer to n (Scheme 1). [b] Data refer to light scattering according to the technique of deGroot and co-workers.[27] [c] Data refer to viscometry according to the technique of deGroot and co-workers.[27] [d] Calculated from the experimental value of g'. [e] Data refer to GPC in *o*-xylenes at 100 °C.

The close correlation between the experimental values of g for the star polymers **4** in Table 2 (0.787 and 0.771) and the theoretical value of $g = 0.778$ for a perfectly regular star polymer supports the assignment of a regular star architecture for the star polymers **4**. For the reactions in Table 2, approximately one-half as opposed to one-third of the initiators led to the formation of star polymers **4** according to the molecular weight discrepancy. Again, the PDIs of the reactions to produce high molecular weight star polymers **4** were low (1.12). Indeed, both ^{1}H NMR and viscometry data for the high molecular weight star polymers **4** provide strong evidence that the star polymers (**4**) produced by the polyhomologation of 1-boraadamantane·THF (**3**) are regular star polymers.

Because extreme care was taken to quantitate the stoichiometric ratios of catalyst **2** to monomer **1**, it appeared that a significant fraction of propagating species terminated and did not result in polymer formation. This presented us with a mechanistic quandary. Following initiation by **2**, approximately two-thirds of the propagating species must effectively terminate (dead catalysts in Table 1) to account for the molecular weight discrepancy. The demise of these propagating species must be rather sudden, because random termination reactions during the course of polymerization would result in a higher polydispersity. Additionally, we speculated that the terminated species occurred at the early stages of polymerization, before a significant fraction of ylide was consumed. Thus, we directed our efforts at examining the products and product distributions at the initial stages of polymerization.

Controlling the first step in this reaction to achieve monohomologation[28] was explored by slowly adding 1 equiv of ylide **1** to a solution of 1-boraadamantane·THF (**2**) in toluene at −78 °C. The resulting white crystalline precipitate was filtered cold, washed with hexanes, and dried under vacuum (0.01 Torr, −60 °C). Upon warming to room temperature under vacuum, the white crystalline solid rapidly melted, exothermically, forming a colorless liquid. The liquid crystallized upon cooling. These observations are consistent with the initial formation and isolation of a solid 1-boraadamantane·ylide complex (**8**) that subsequently undergoes a [1,2]-migration upon warming to room temperature. The decomposition of complex **8** proceeds under ambient conditions, and the expelled DMSO is captured to form 1-borahomoadamantane·DMSO (**9**) (Scheme 4).

Complex **9** sublimes (0.01 mmHg, 75 °C) and was isolated in 65% yield. The structure of **9** was confirmed by X-ray crystallography (Figure 3).

(21) Busch, B. B.; Paz, M. M.; Shea, K. J.; Staiger, C. L.; Stoddard, J. M.; Walker, J. R.; Zhou, X. Z.; Zhu, H. *J. Am. Chem. Soc.* **2002**, *124*, 3636.
(22) Burchard, W. *Adv. Polym. Sci.* **1999**, *143*, 113.
(23) (a) Zimm, B. H.; Stockmayer, W. H. *J. Chem. Phys.* **1949**, *17*, 1301. (b) Berry, G. C.; Orofino, T. A. *J. Chem. Phys.* **1964**, *46*, 1614.
(24) (a) Drott, E. E.; Mendelson, R. A. *J. Polym. Sci., Part A-2* **1970**, *8*, 1361. (b) Drott, E. E.; Mendelson, R. A. *J. Polym. Sci., Part A-2* **1970**, *8*, 1373.
(25) Zimm, B. H.; Kilb, R. W. *J. Polym. Sci.* **1959**, *37*, 19.
(26) Hadjichristidis, N.; Xenidou, M.; Iatrou, H.; Pitsikalis, M.; Poulos, Y.; Avgeropoulos, A.; Sioula, S.; Paraskeva, S.; Velis, G.; Lohse, D. J.; Schulz, D. N.; Fetters, L. J.; Wright, P. J.; Mendelson, R. A.; García-Franco, C. A.; Sun, T.; Ruff, C. J. *Macromolecules* **2000**, *33*, 2424.
(27) Wood-Adams, P. M.; Dealy, J. M.; deGroot, A. W.; Redwine, O. D. *Macromolecules* **2000**, *33*, 7489.
(28) Stoddard, J. M.; Shea, K. J. *Organometallics* **2003**, *22*, 1124.

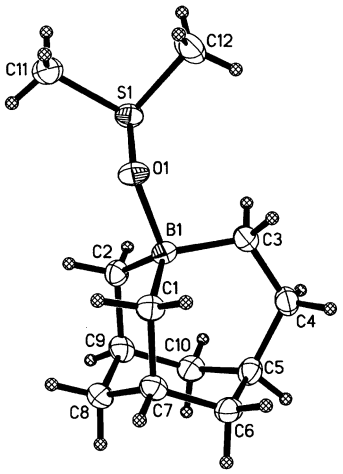

Figure 3. The X-ray crystal structure of 1-borahomoadamantane·DMSO (**9**).

There have been earlier efforts to homologate 1-boraadamantane. The monohomologation of 1-boraadamantane was previously attempted with trimethylamine methylide. The primary product, 1-borahomoadamantane·trimethylamine, proved difficult to separate from the nonhomologated 1-boraadamantane·trimethylamine formed as a byproduct of the reaction.[29] Interestingly, Mikhailov and co-workers previously prepared a 1-boraadamantane·methylenetriphenylphosphorane complex which was stable to 180 °C.[30] However, the monohomologation of 1-boraadamantane by triphenylphosphine methylide could not be accomplished because of thermal decomposition prior to migratory insertion.[31] Thus, the successful monohomologation of 1-boraadamantane depends not only on the facility with which the leaving group departs, but also on the degree to which the ylide remains bound to boron under a given set of conditions for [1,2]-migration. The monohomologation of 1-boraadamantane by dimethylsulfoxonium methylide (**1**) is a rather unique reaction because it readily transpires from the solid state, and, most importantly, it results in the controlled monohomologation of a trialkylborane[32] by ylide **1**.

Compound **9** is readily oxidized with TAO, providing *cis*-1-hydroxyethyl-3,5-bis(hydroxymethyl)cyclohexane (**10**) in 87% isolated yield (Scheme 5).

The low molecular weight oxidized products were acetylated prior to being assayed by GC. Acetylation of triols **7** and **10** provide the acetylated triols **11** and **12** in 83% and 86% yield, respectively.

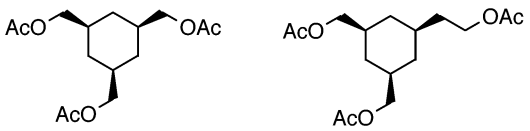

11 **12**

With the GC standards **11** and **12** in hand, identification of the products from multiple homologations was facilitated. For example, in an attempt to effect the monohomologation of 1-borahomoadamantane, 1 equiv of ylide **1** was added to a solution of 1-borahomoadamantane·DMSO (**9**) in toluene at −50 °C. The reaction mixture was allowed to warm to room temperature with stirring. Following consumption of ylide **1**, oxidation of the products was accomplished by refluxing with TAO. After separation by perparative TLC, triols **10**, **13a**, and **14a** were identified as the products of the reaction, and their structures were determined by ^{1}H NMR and ^{13}C NMR (D_2O). The relative distribution of the three triols **10**, **13a**, and **14a** was obtained by GC analysis of the triacetates **12**, **13b**, and **14b** (Scheme 6).

Scheme 4

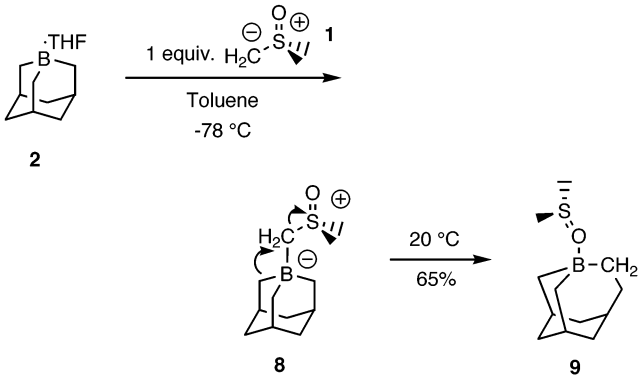

Scheme 5

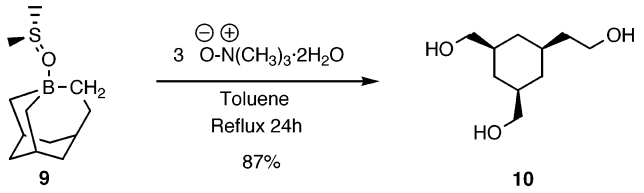

Triol **10** arises from the oxidation of the remaining 1-borahomoadamantane **9**, and triols **13a** and **14a** arise from the oxidation of the triorganoboranes **15** and **17**, respectively (Figure 4).

In the first homologation of the 1-borahomoadamantane core, formation of the organoborane species **15** is strongly favored over the formation of **16**. Similarly, in the subsequent homologation of **15**, species **17** is formed exclusively over **18**.

The GC spectrum of the triacetates **12**, **13b**, and **14b** from the reaction depicted in Scheme 6 is shown in Figure 5.

The triacetates **12**, **13b**, and **14b** appear at retention times of 18.5, 19.4, and 20.3 min in 26%, 43%, and 31% composition, respectively. GC-MS under chemical ionization (CI) conditions provided the corresponding masses $(M + NH_4)^+$ of the triacetates **12**, **13b**, and **14b** as 332, 346, and 360 *m*/*z*, respectively. The minor peak at the retention time of 19.5 min has been tentatively assigned to the triacetate formed upon oxidation and acetylation of the trialkylborane (**16**), because it also has a mass (CI) of 346 *m*/*z*. Because the side peak at 19.5 min accounts for less than 2% of the total reaction products, **16** is the disfavored product of the second [1,2]-migration. Triacetates **13b** and **14b** were separated by column chromatography and were characterized by ^{1}H NMR and ^{13}C NMR ($CDCl_3$).

The ^{1}H NMR spectra of triols **7**, **10**, **13a**, and **14a** are shown in Figure 6.

(29) Mikhailov, B. M.; Govorov, N. N.; Angelyuk, Ya. A.; Kiselev, V. G.; Struchkova, M. I. *Izv. Akad. Nauk SSSR, Ser. Khim.* **1980**, *29*, 1621.
(30) Sergeeva, M. V.; Yanovskii, A. I.; Struchkov, Yu. T.; Mikhailov, B. M.; Gurskii, M. E.; Pershin, D. G. *Izv. Akad. Nauk SSSR, Ser. Khim.* **1985**, *34*, 2483.
(31) Gurskii, M. E.; Pershin, D. G.; Mikhailov, B. M. *J. Organomet. Chem.* **1984**, *260*, 17.
(32) (a) Tufariello, J. J.; Lee, L. T. C. *J. Am. Chem. Soc.* **1966**, *88*, 4757. (b) Goddard, J.; Le Gall, T.; Mioskowski, C. *Org. Lett.* **2000**, *2*, 1455.

Scheme 6

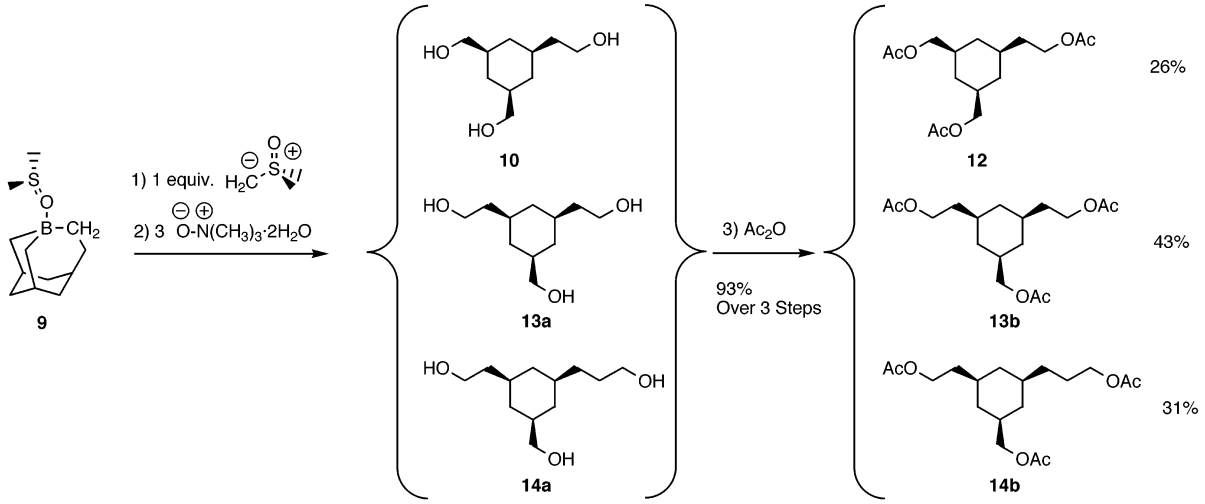

The pseudosymmetry of the equatorial and axial protons of the triols at 1.80 and 0.60 ppm, respectively, degrades as the asymmetry of the triols increases. In the ^{1}H NMR spectrum of polymeric triol **4** (Figure 2), the return of the equatorial and axial protons to pseudosymmetry and the observed triplet of the equivalent hydroxymethylene terminal groups are features consistent with similar polymer arm lengths and the proposed regular star architecture.

The experimental outcome of the addition of 1 equiv of ylide **1** to 1-borahomoadamantane·DMSO (**9**) is remarkable for two reasons. First, it was anticipated that the analysis of products resulting from the reaction of **9** with 1 equiv of ylide **1** would show a distribution of triacetates arising primarily from the oxidation and acetylation of species **15** and **16**. Second, only minor amounts of the triacetates arising from either the starting 1-borahomoadamantane **9** or species **17**, **18**, and **19** were anticipated. The experimental results, however, showed that a substantial amount of the 1-borahomoadamantane starting material remained (26%) after the consumption of 1 equiv of ylide. Further, the homologation of 1-borahomoadamantane proceeds almost exclusively to form species **15** (41%) over species **16** (2%), and the subsequent homologation of **15** proceeds exclusively to form organoborane **17** (31%). The selective formation of **15** and **17** and the distribution of **15**, **17**, and remaining the 1-borahomoadamantane **9** strongly suggest that the reaction pathways have substantially different activation energies with ylide resulting in a path-selective sequence of homologation. Molecular modeling of the trialkylborane·ylide complexes of **9**, **15**, and **17**, and their associated [1,2]-migration transition state energies leading to isomeric tricyclic organoboron compounds, provides useful insight into the observed pathway and will be subsequently examined in detail.

Both the monohomologation of 1-boraadamantane to give 1-borahomoadamantane **9** and the highly selective subsequent two homologations of **9** reveal a change in the reactivity of the tricyclic organoborane compounds. Nevertheless, the first three generations of tricyclic organoboron compounds formed by homologation of 1-boraadamantane contain active Lewis acidic centers for polymerization, and, as yet, no evidence for terminated species was found. Thus, we continued to search for evidence for termination at the early stages of polymerization.

Insight into the termination of certain intermediates came from a polymerization (Scheme 1) conducted with an initial (1/3)-ylide:boraadamantane ratio of 27. After oxidation and repre-

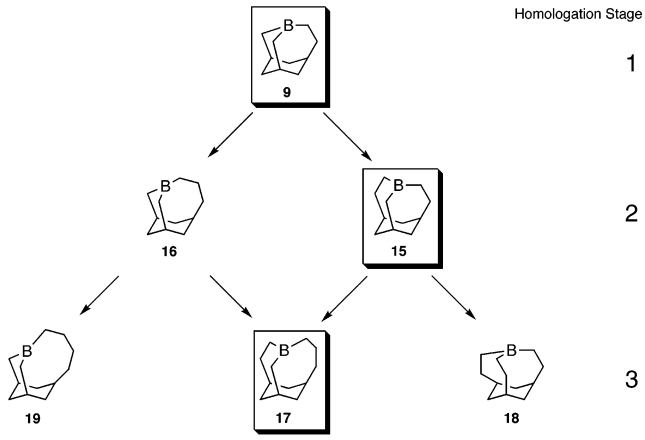

Figure 4. Products from the first three homologations of 1-boraadamantane by ylide **1**.

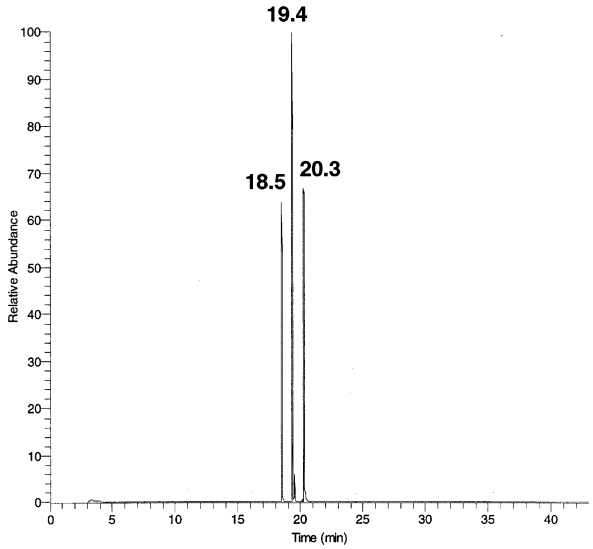

Figure 5. The GC chromatograph of triacetates **12**, **13b**, and **14b** formed from the reaction shown in Scheme 6.

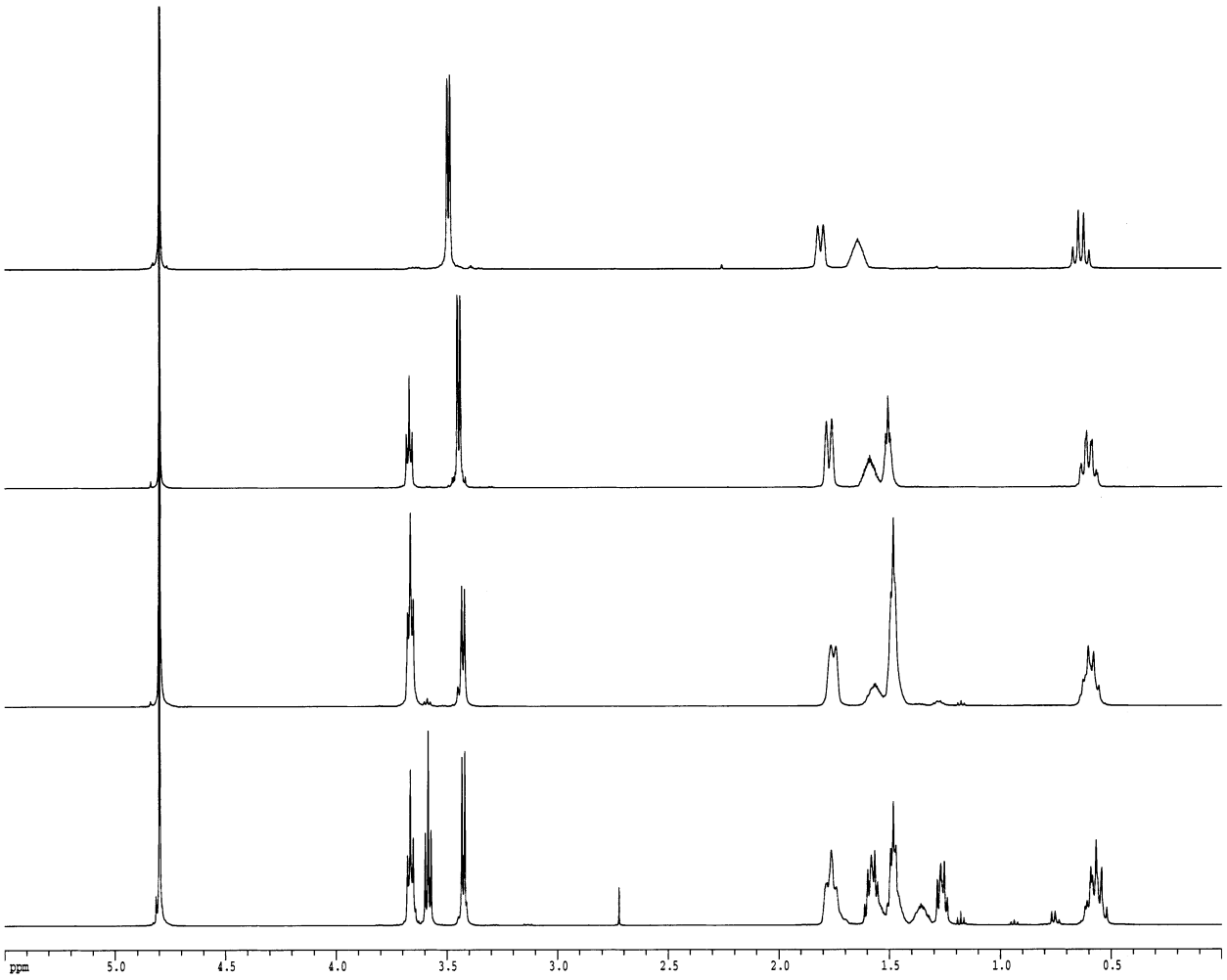

Figure 6. The ^{1}H NMR (500 MHz, D_2O) of triols **7**, **10**, **13a**, and **14a** in descending order.

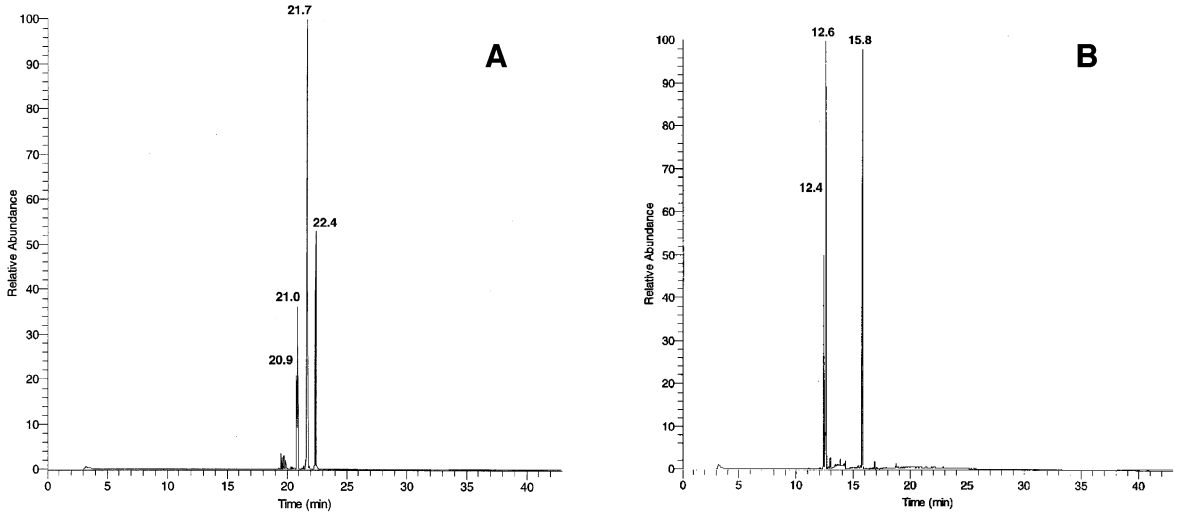

Figure 7. (A) The GC chromatograph of acetylated triols produced by the oxidation of terminated species. (B) The GC chromatograph of the "terminated" trialkylboranes.

cipitation, polymer **4** was isolated in 93% yield. The polymer's DP was observed to be 100 by GPC with a polydispersity of 1.08. The filtrate from reprecipitation and washing of the polymer was found by TLC to contain a distribution of triols with R_f values similar to that of **10**. The triols were acetylated by heating with excess acetic anhydride at 100 °C, followed by purification by column chromatography. The GC chromatograph of the acetylated triols revealed a total of five compounds (Figure 7A).

GC-MS reveals two triacetates at 20.9 and 21.0 min, both with masses of 374 *m*/*z* (CI) corresponding to a total DP of 4 and accounting for 14% of the terminated species. In addition,

Scheme 7

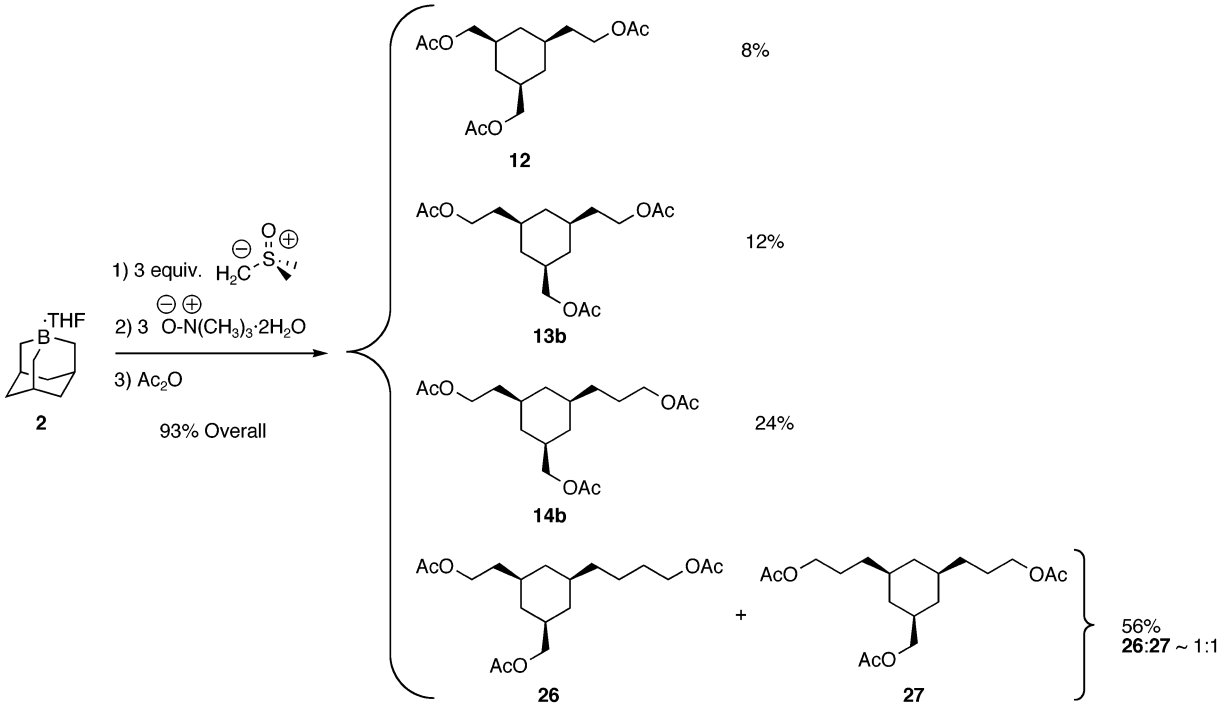

the peak at 21.7 min contained two triacetates, both with masses of 388 *m*/*z* (CI) corresponding to a total DP of 5. These species amount to 51% of the terminated catalysts. Finally, there is one triacetate appearing at 22.4 min that has a mass of 402 *m*/*z* (CI) corresponding to a total DP of 6 and accounting for 35% of the terminated species. The total mass of the acetylated triols accounts for 63% of the initiator used in the polymerization.

The species with a retention time of 22.4 min in Figure 7A was separated by column chromatography. The ^{1}H NMR ($CDCl_3$) spectrum of this triacetate includes a triplet at 4.07 ppm (J = 6.8 Hz, 4H) and a doublet at 3.89 ppm (J = 6.4 Hz, 2H) corresponding to the ester methylenes. The ^{13}C NMR spectrum of this compound shows a total of 13 carbon peaks. The compound was thus identified as the triacetate **20** by ^{1}H and ^{13}C NMR ($CDCl_3$).

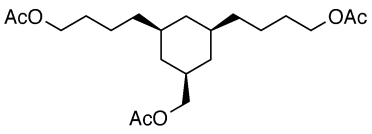

20

Additionally, the species appearing in the peak at 21.7 min in Figure 7A were separated by column chromatography and identified as a 1:1 mixture of triacetates **21** and **22** by ^{1}H NMR and ^{13}C NMR.

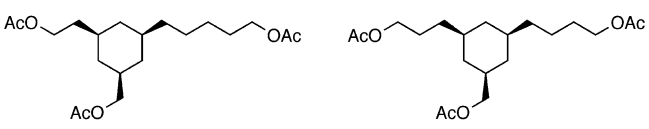

The triacetates **20**, **21**, and **22** arise from the oxidation and acetylation of the triorganoboranes **23**, **24**, and **25**, respectively.

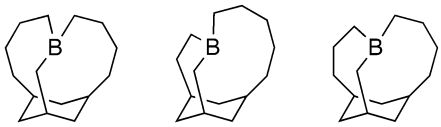

Direct spectroscopic evidence for the terminated triorganoboranes **23**, **24**, and **25** was obtained by conducting a polymerization similar to trial 1 in Table 1, removing solvents in vacuo and filtering off the polymer on a plug of silica. The GC chromatograph of the filtrate reveals three low molecular weight components (Figure 7B). EI-GC TOF-MS established the peaks at 12.4 and 12.6 min to have masses of 204.2057 and 204.2039 *m*/*z* (EI, calcd for $C_{14}H_{25}B$: 204.2049) corresponding to triorganoborane species with a total DP of 5. The compounds are present in roughly a 1:1 ratio as determined by ^{1}H NMR. The peak at 15.8 min was found to have a mass of 218.2202 *m*/*z* (EI, calcd for $C_{14}H_{25}B$: 218.2202) corresponding to a total DP of 6. The minor species with a total DP of 4 were not observed after filtering through silica.

Additional experiments were conducted to elucidate the sequence of events at the early stages of polyhomologation. After the addition of 3 equiv of ylide **1** to a solution of 1-boraadamantane·THF (**2**), followed by oxidation and acetylation, a mixture of triacetates was obtained in 93% yield (Scheme 7).

The GC chromatograph of the triacetates produced in the reaction shown in Scheme 7 reveals a distribution of five products arising from one to four homologations, with no products resulting from five homologations (Figure 8A).

Triacetates **12**, **13b**, and **14b** were identified by their retention times and associated masses from GC-MS. The products of four

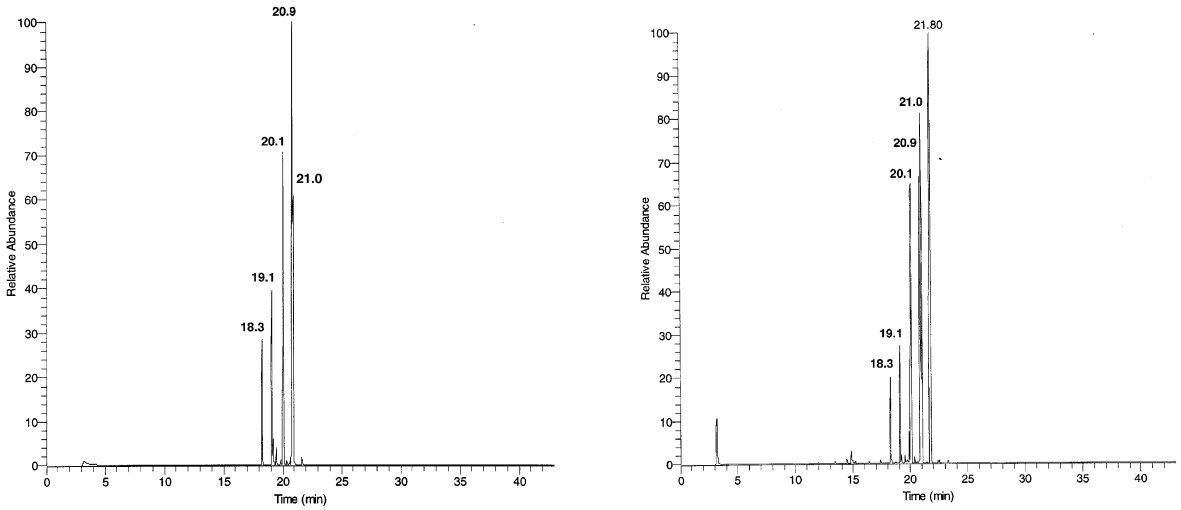

Figure 8. (A) The GC chromatograph of the triacetates produced by the reaction of 3 equiv of **1** with 1-boraadamantane·THF (**2**) followed by oxidation and acetylation. (B) The GC chromatograph of the triacetates produced by the reaction of 4 equiv of **1** with 1-borahomoadamantane·DMSO (**9**) followed by oxidation and acetylation.

Scheme 8

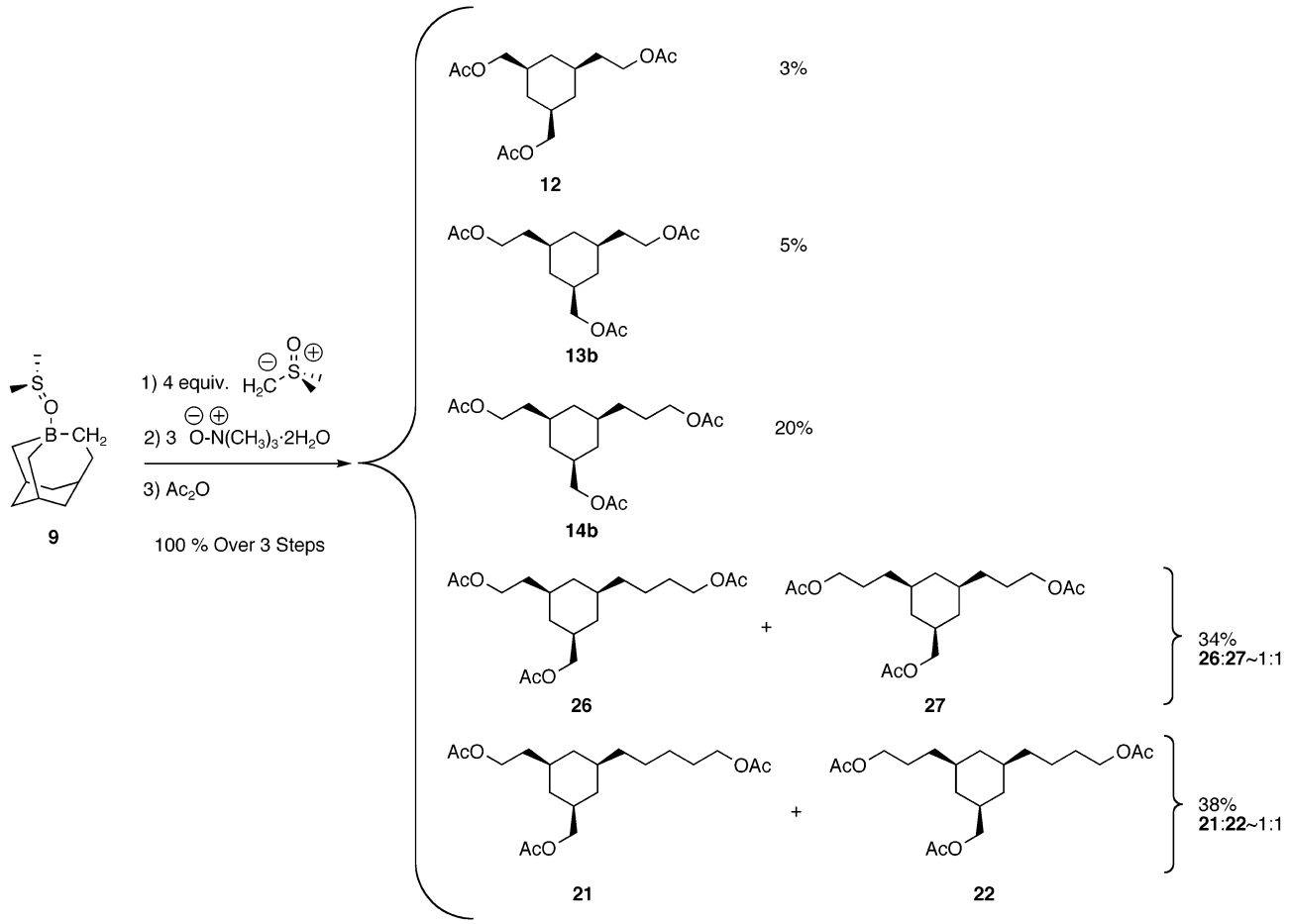

homologations in Figure 8A appearing at retention times of 20.9 and 21.0 min were separated from triacetates **12**, **13b**, and **14b** by column chromatography and identified as a mixture of triacetates **26** and **27** by ^{1}H NMR and ^{13}C NMR. The preceding results offer a clear indication that an energetic barrier exists between the fourth and fifth homologation steps.

In a similar experiment, this time adding 4 equiv of ylide **1** to a solution of 1-borahomoadamantane·DMSO **9**, followed by oxidation and acetylation, a mixture of seven triacetates was obtained in quantitative yield (Scheme 8).

The distribution contains products arising from one to five homologations of the 1-boraadamantane core, with no products resulting from six homologations (Figure 8B). This result indicates that an energetic barrier exists between the fifth and sixth homologation of 1-boraadamantane as well. All seven triacetates were identified by their retention times. No evidence

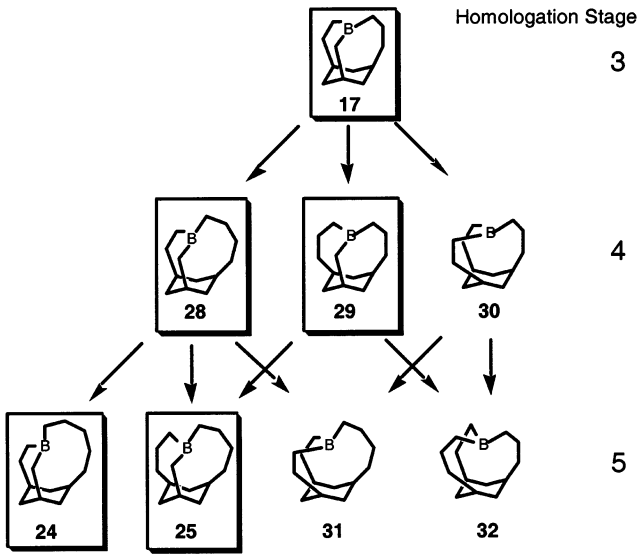

Figure 9. Products (outlined) arising from two homologations of trialkylborane **17** with ylide **1**.

was found for products with a total DP of 5 other than triacetates **21** and **22**. The identification of the triacetates in the reaction shown in Scheme 8 demonstrates that species **17** only gives rise to the organoboranes **28** and **29**, which give rise directly to organoboranes **24** and **25**, respectively. Thus, the pathways of polymerization from three homologations to five homologations of the 1-boraadamantane core have been experimentally determined (Figure 9).

Interestingly, by the fifth homologation stage of the polyhomologation of 1-boraadamantane, the only two organoborane species with a total DP of 5 observed are the same species that are observed to be the major component of the two-thirds terminated catalysts. These results led to speculation that the one-third propagating catalysts must arise from the organoborane species **24**, because species **25** leads directly to species **26** which is also found in the residual two-thirds terminated catalysts.

To give experimental supporting evidence to the theory that **24** is the species through which polymerization proceeds, the isolated trialkylboranes **23**, **24**, and **25** were resubjected to ylide **1** and subsequently oxidized under the normal polyhomologation protocol. According to the observed DP (GPC) of the polymer recovered, one-third of the two-thirds residual trialkylboranes **23**, **24**, and **25** react to give a star polymer **4** with a PDI of 1.04 upon this second exposure to ylide. This result implies that at least one of the residual trialkylboranes **23**, **24**, or **25** is more active than the remaining two. Examining the species resulting from the oxidation and acetylation of the residual boranes after the second exposure to ylide **1**, we should expect to see a predominance of triacetate **20** and **22**, if the borane leading to the triacetate **21** is largely consumed upon reexposure to ylide. In the GC chromatograph of the triacetates produced by this experiment, we do observe an enrichment of triacetate **20** (49% composition) and a depletion of triacetates **21** and **22** (47% total composition). Additionally, the ratio of triacetates **21**:**22** drops from 1:1 after the first exposure to ylide to 1:3 after the second exposure to ylide. These results strongly suggest that species **24** is the primary contributor to the active one-third catalytic species that continue to propagate and result in polymer formation.

Scheme 9

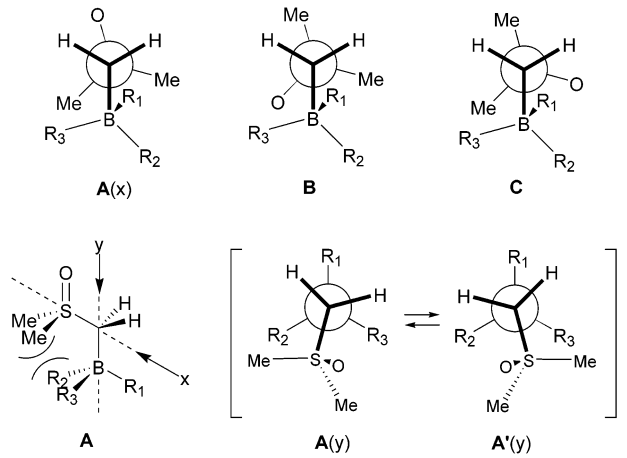

Computational Studies

Because of the complexity of the branching pathways that are available to propagating species in the polyhomologation of 1-boraadamantane, a modeling study of each trialkylborane species and branching pathway was undertaken in an effort to corroborate and extend the experimental findings. From 1-boroadamantane, which contains all six-membered rings, the tricyclic boranes examined by modeling consist of 6- to 13-membered rings. The size of the rings expands from the common to medium to large rings. It is of interest that many of the tricyclic boranes that experience severe transannular ring strains, such as species **23**−**25**, **28**, and **29**, fall in the medium-sized range of rings. In the computational study, the ground-state conformations of the free trialkylborane species were first optimized. Next, the energy of complex formation between the free trialkylborane species with ylide **1** was calculated. Finally, the energies of transition states leading to the different, isomeric trialkylboranes were assessed to elucidate the lowest energy pathways of polymerization.

Although acyclic trialkylboranes have a flat geometry utilizing the sp^2 hybrid orbitals of boron, cyclic trialkylboranes may experience pyramidalization because of geometrical restrictions. The boron centers in 1-boraadamantane, 1-borahomoadamantane, and other smaller tricyclic boranes show a calculated outward pyramidalization. Larger boracycles such as **23**−**25**, **28**, and **29**, however, show a flat or inward pyramidalization at the boron center. The inward distortion of bridgehead boron centers for larger boracycles reduces the transannular and angle strain present in medium and large multicyclic rings. The $\theta_{\sigma p} - 90°$ value for inward pyramidal distortions of the HF/3-21G* geometry optimized structures ranges from 2.0° for **28** to 4.6° for **23**. The boron centers of these systems should be less Lewis acidic, because the formation of a borate complex requires outward pyramidalization. The outward rehybridization exacerbates transannular strain, which further destabilizes complex formation for these inward pyramidal species.

As an initial survey of possible ylide borane constructs for computational studies, trimethylborane ylide complexes were examined. The lowest energy conformation of the trimethylborane-dimethylsulfoxonium methylide complex is shown schematically as **A** in Scheme 9. The substituents at sulfur and boron are slightly twisted from the staggered conformation. The other rotational isomers **B** and **C**, although seemingly less sterically

hindered, were found to be less stable at all levels of computational theory used in the study. The energy differences between **A**, the most stable form, and **B** were 3.52, 4.68, and 5.02 kcal/mol at the 3-21G*/3-21G*, 6-31G*/6-31G*, and B3LYP/6-31G* levels of theory, respectively. Conformation **C** is 3.60 kcal/mol higher in energy than **A** at the 3-21G*/3-21G* level of theory. The anti oriented S−O bond to the CH_2−B can effectively stabilize the negative charge associated with the borate component. Conformations resembling **A**, therefore, were used for the calculation of transition state energies and complex formation energies for the trialkylborane·ylide complexes of 1-boraadamantane and its homologated boranes.

Even after the structure of the complex was restricted to conformation **A**, a total of six conformations could exist for each complex formed with an asymmetric borane. As shown by **A**(*y*) and **A′**(*y*) in Scheme 9, for asymmetric boranes there are two possible conformational isomers with the sulfoxide portion anti to each different alkyl group. All six conformations were examined for each asymmetric borane to determine the lowest energy conformation. A summary of the energies of complex formation and the transition state energies for each trialkylborane species produced during the first seven homologations of 1-boraadamantane is illustrated in Figure 10.

The calculations reveal that the transition state energies, defined as $E_{TS} = E$(transition state) − E(complex), of the lowest energy transition state at each homologation stage did not change significantly whereas the energy of complex formation was much more variable. For convenience, matrix notation is used in addition to compound numbers when referring to a particular trialkylborane to specify a given isomer at a given homologation stage. In this system of notation, the 1-boraadamantane cage is denoted as the [0.0.0] organoborane, and the 1-borahomoadamantane cage is denoted as the [1.0.0] species. A maximum difference of 4 kcal/mol was found between the [0.0.0] 1-boraadamantane system (E_{TS} = 18.82 kcal/mol) and the [2.2.0] system (**29**) (E_{TS} = 14.82 kcal/mol). The transition state energy is found to decrease as the ring size increases, with minima occurring at both the fifth and the sixth homologation stages. This trend is opposite to the trend in complexation energy which increases with the homologation stage, reaching a maximum at the fifth and sixth homologation stages. Systems with low transition state energies are aided by the partial relief of strain from the tetravalent borate complex to the transition state that has a flattened trialkylboranyl ring portion. An illustration of the complexation of a strained tricyclic borane is shown in Figure 11.

The calculated values of transition state energies summarized in Figure 10 enabled the mapping and comparison of the different modes of the polyhomologation of 1-boraadamantane until the eighth stage. Thick solid arrows in Figure 10 represent the probable reaction flow where the competing isomeric transition states have more than 2 kcal/mol higher energy. After branching at the second and third stages of homologation, three probable homologation paths were identified as energetically feasible to lead to products at the fourth stage of homologation. Experimentally, however, branching was not observed at the second stage of homologation, although, in the experimentally observed pathway of homologation, branching from the third stage of homologation matched perfectly with one of the two energetically reasonable pathways elucidated by modeling. Estimation of activation energies for the pathways of homologation is helpful to compare the time-dependent reaction progress and rationalize the observed products and product distributions. From the calculations, the reaction energy profiles varied depending on the homologation stage as shown in Figure 12.

The reaction in which 1 equiv of ylide **1** is added to 1-boraadamantane (Scheme 4) resulting in a single product of monohomologation is best described by the energy profile in Figure 12a. The subsequent second, third, and fourth stages of homologation have energy profiles best represented by the profile in (b). Therefore, addition of 1 equiv of ylide **1** to 1-borahomoadamantane leads to product mixtures comprised of unreacted, mono-, and polyhomologated products. The energy profile in (b) is the same profile that applies to the parent reaction with trimethylborane. The energy profiles for the fifth, sixth, and seventh homologation stages resemble the profile shown in (c). For the fifth through seventh homologation stages, the energy of complex formation (E_C) is positive, and the activation energy for those systems is the sum of E_{TS} and E_C. For the eighth stage of homologation and subsequent homologations, the energy profiles return to resemble the profile in (b). Further stages in homologation will have energy profiles of type (b), because the cyclic boranes containing very large rings should behave like acyclic alkyl boranes.

The calculated activation energies thus obtained were plotted for the three energetically possible reaction paths in Figure 13 to elucidate which pathway is the probable pathway for active catalysts.

While the activation energy barriers remain relatively steady until the fourth homologation stage, the activation energies in all pathways increase for the fifth, sixth, and seventh stages of homologation. It is evident that the reaction via the [2.2.1] species (**32**) leading to the [2.2.2] species cannot be an actual polymerization path because of a calculated energy difference of 10.3 kcal/mol from the lowest energy path via the [5.1.0] organoborane (**33**). The path via the [3.3.0] species (**23**) also has an energy difference 3.4 kcal/mol higher than that via the [5.1.0] system (**33**). We believe this energy difference is high enough to produce the observed selectivity. The polyhomologation with 1-boraadamantane, therefore, likely proceeds via the [4.1.0] species (**24**) to the [5.1.0] organoborane (**33**) to the [6.1.0] species (**34**), ultimately leading to the propagating catalysts. The low activation energy for the homologation with the [6.1.0] borane (**34**), 16.27 kcal/mol, suggests that strain is relieved and further homologations will have similarly low activation energies or, at most, energies close to those for the homologation with trimethyl borane (18.4 kcal/mol).

If a fraction of propagating species pass through the fifth to seventh homologation stages, then the remaining unreacted boranes would compete with the higher homologated boranes having relatively low activation energies. If we assume an activation energy of 18.4 kcal/mol for the polymerizing homologation reactions, the values of 24.29 kcal/mol for the [3.3.0] system (**23**) are 5.9 kcal/mol higher. Kinetic simulation for a simple competing polymerization reaction in which a 3 kcal/mol difference in activation energy for competing reactants was imposed shows that roughly 83% and 74% of unfavorable reactants remain after reacting with 20 and 40 equiv of ylide, respectively, at 298 K. Imposing a 5 kcal/mol difference in the

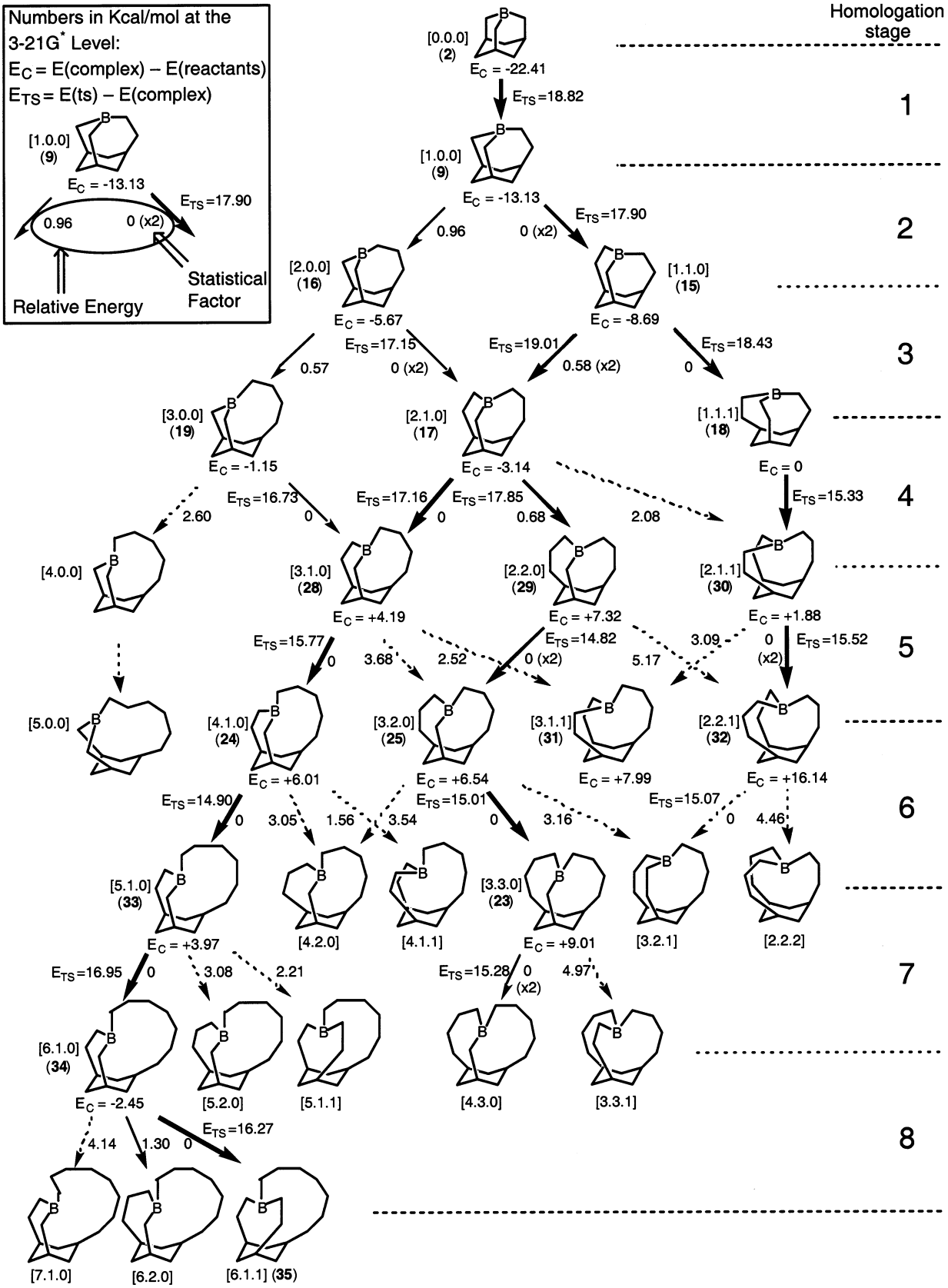

Figure 10. Results of a molecular modeling study of the initial stages of the polyhomologation of 1-boraadamantane·THF.

simulation leads to 98% and 96% of unfavorable reactants remaining after reaction with 40 and 100 equiv of ylide, respectively, at 298 K. Thus, a significant fraction of the [3.3.0] borane (**23**) and other five-carbon homologated boranes such as [4.1.0] (**24**), [3.2.0] (**25**), and [2.2.1] (**32**) could plausibly survive the conditions of the polyhomologation reaction.

It is of interest whether further homologations would also proceed selectively past the eighth stage of homologation. One

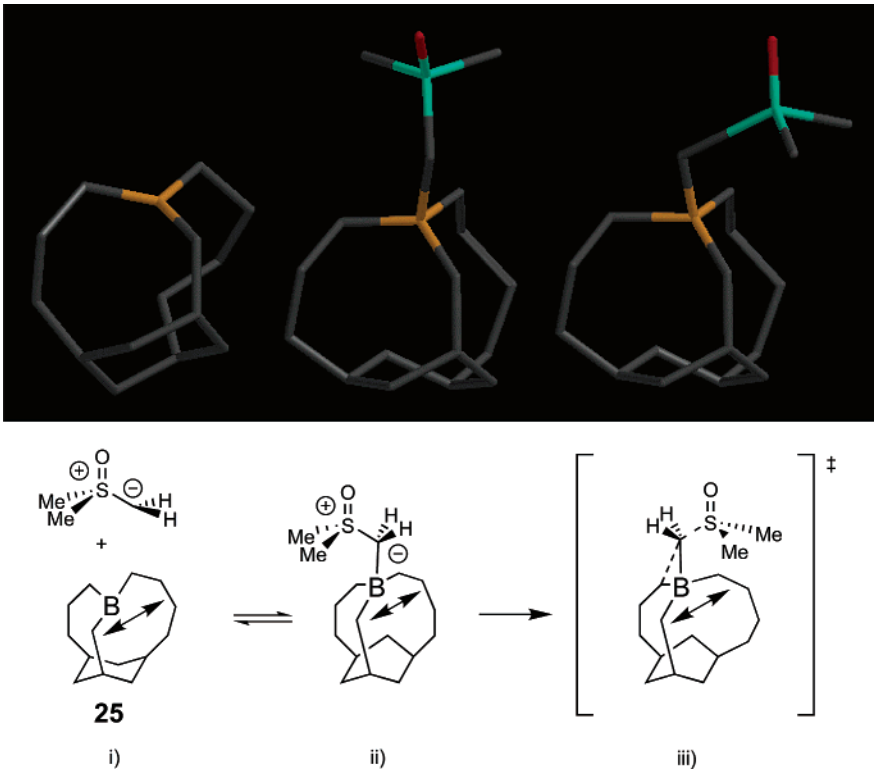

Figure 11. An illustration of the [3.2.0] system (**25**), its complex, and transition state structures. (i) Tricyclic boranes at the fourth through sixth homologated stages contain boron centers with inward pyramidalization to reduce transannular interaction and angle strain. (ii) The boracycles are destabilized due to the complex formation with the ylide **1**. (iii) Transannular strain energy is partially relieved at the transition state.

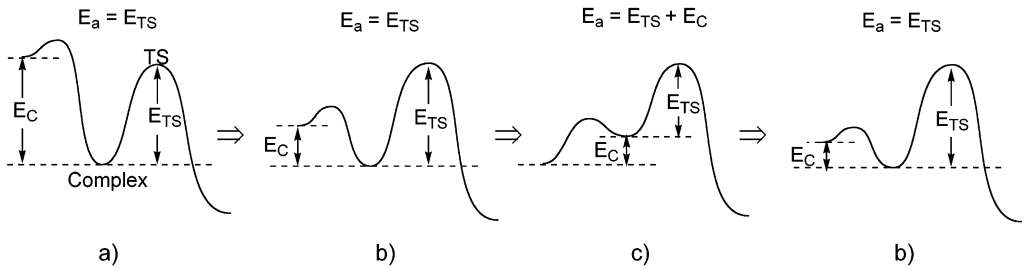

Figure 12. The changing energy profiles of complexation and subsequent homologation describing different stages among the first through eighth homologation stages.

might expect polyhomologation to proceed only along one or some selected paths considering the computational results for the first through eighth stages of homologation. The homologation reactions with cyclic boranes containing large rings, however, take place rather randomly, because large cyclic boranes such as the [6.1.0] species (**34**) and the [6.1.1] organoborane (**35**) have several conformational isomers with ylide **1** similar in energy to the lowest energy isomer. Inevitably, this causes the transition energies for the three regioisomeric trialkylborane·ylide complexes to be closer. The actual structure of the polymer (**4**) is not highly symmetric even with the random homologation after the eighth or ninth homologation stage, because the probable borane formed after the eighth homologation step, the [6.1.1] borane (**23**), has one arm longer by five carbons. However, in the limit of making large polymers, this difference becomes insignificant, and a fairly symmetric, regular star polymer **4** is expected.

Conclusions

1-Boraadamantane·THF (**2**) can be used as an initiator for polyhomologation to give rise to macrotricyclic trialkylborane structures **3**. The macrotricyclic species **3** may be further elaborated by oxidation to regular star polymers **4** of low PDI. Discrepancies between the calculated and observed molecular weight of **4** led to a detailed mechanistic study of the initial stages of polyhomologation. In the mechanistic study, 1-borahomoadamantane·DMSO (**9**) was synthesized by the controlled monohomologation of 1-boraadamantane·THF (**2**) with ylide **1**. A high degree of selectivity in the second and third stages of homologation was also observed.

After a polymerization experiment, the discrepancy between the theoretical and observed polymer molecular weight was established by isolating and identifying the two-thirds of trialkylborane species that did not result in polymer formation. Because the two-thirds residual trialkylboranes occurred at the fifth and sixth stages of homologation, further homologation experiments were conducted to probe the initial stages of polyhomologation. These experiments showed that no additional species were produced in addition to the ones that were isolated and identified as the residual boranes. Molecular modeling corroborated this observation because estimates of the lowest

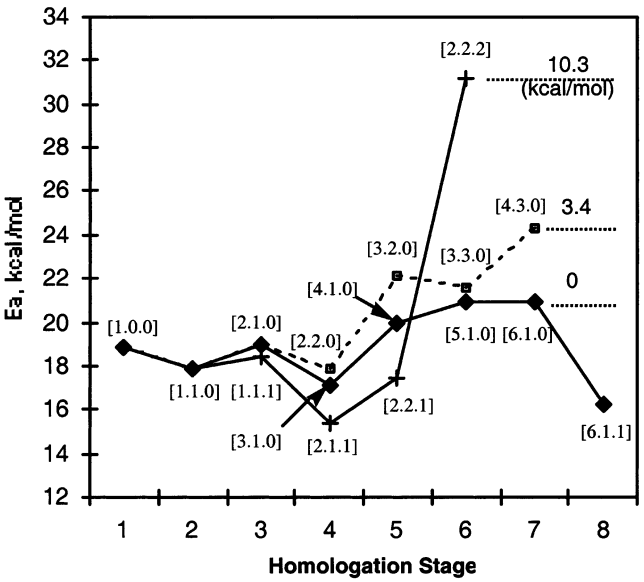

Figure 13. A plot of activation energies for three different pathways at the initial stages of polyhomologation. The data point labeled [1.0.0] represents the transition state energy for the homologation of the [0.0.0] species.

energy pathway for polymerization and kinetic simulation showed that polymerization could proceed through the boranes that were isolated as residual boranes after polyhomologation.

In accordance with the model, we hypothesized, tested, and demonstrated that a large fraction of the one-third active propagating species species that ultimately results in polymer formation proceeds through the [4.1.0] trialkylborane (**24**). According to the model, the lowest energy pathway for the homologation of **24** transpires to give the [5.1.0] triorganoborane (**33**) followed by the [6.1.0] (**34**) and finally the [6.1.1] trialkylborane (**35**), after which each branch on the cyclohexane core participates in polyhomologation. During each polymerization, it is curious that only one-third of the propagating species result in polymer formation and, further, that those propagating species largely proceed through **24** and yet there is a fraction of **24** that remains intact after polymerization. However, molecular modeling and kinetic simulation support this scenario in an analysis of the pertinent geometrical, energetic, and kinetic factors contributing to the loss of activity in the tricyclic boranes of medium ring size. Additionally, the second exposure of ylide to boranes **23**, **24**, and **25** showed a substantial depletion of borane **24** relative to **23** and **25**, strongly supporting the lowest energy pathway elucidated by molecular modeling.

Experimental Section

Instrumentation. All ^{1}H NMR spectra were acquired at 400 or 500 MHz on Bruker spectrometers. Chemical shifts (δ) are listed in ppm against deuterated solvent peaks as an internal reference. Coupling constants (J) are reported in hertz, and the abbreviations for splitting include: s, single; d, doublet; t, triplet; q, quartet; p, pentet; m, multiplet; br, broad. All ^{13}C NMR spectra were acquired on Bruker instruments at 125.8 MHz. Chemical shifts (δ) are listed in ppm against solvent carbon peaks as an internal reference. All ^{11}B NMR spectra were acquired at 237 MHz on a Bruker spectrometer. All chemical shifts (δ) are listed in ppm against boron trifluoride etherate as an external reference. Infrared spectra (IR) were assayed on a Perkin-Elmer 1600 Series FTIR spectrometer. GPC was conducted on a Waters 150-C Plus Gel permeation chromatograph. High-resolution mass spectra (EI, hexanes) were recorded using either a VG 7070e high-resolution mass spectrometer or a Fisons Autospec mass spectrometer. Differential scanning calorimetry (DSC) was conducted on a Dupont Thermal Analyst 2000 with a 910 DSC module at a 10 °C/min heating rate under a N_2 atmosphere with an aluminum oxide reference. Melting points were assayed on a Thomas-Hoover capillary melting point apparatus.

General Procedures. Tetrahydrofuran, methylene chloride, diethyl ether, and benzene were dried by filtration through alumina according to the procedure described by Grubbs.[33] All other solvents were distilled from CaH_2 prior to use. Boron trifluoride etherate (BF_3·Et_2O, Aldrich) was distilled over CaH_2 under reduced pressure (20 mmHg, 65 °C). Allyl bromide (Aldrich) was distilled over CaH_2. All reactions were run in flame-dried glassware under a positive N_2 or argon atmosphere. Removal of volatile solvents transpired under reduced pressure using a Büchi rotary evaporator and is referred to as removing solvents in vacuo. Thin-layer chromatography was conducted on precoated (0.25 mm thickness) silica gel plates with 60F-254 indicator (Merck). Column chromatography was conducted using 230−400 mesh silica gel (E. Merck reagent silica gel 60).

Computational Methods. All calculations were performed by Silicon Graphics workstations. Molecular mechanics calculations were carried out using MacroModel (version 7.0). Ab initio calculations were performed by Spartan[34] (version 5.0) and Gaussian 98[35] (revision A.11) programs. Spartan software was used for structural modifications, whereas Gaussian 98 was used for energy and frequency calculations. The first step for finding the energies of conformational isomers for the cyclic boranes and the ylide complexes was the conformational search for the corresponding cycloalkanes. The molecular mechanics conformational searching routine imbedded in MacroModel software was utilized with the MM3 force field. Conformations within 2 kcal/mol were transferred to Spartan software and fully optimized at the HF/3-21G* level of theory. The structures of the lowest energy conformations were essentially the same regardless of computational levels with MM3 molecular mechanics or HF/3-21G*. The lowest energy conformations thus obtained were used as the basic skeletons for constructing the borate complexes. The ylide-borate complex had mostly six different conformations depending on the orientations of the ylide portion (see Discussion section). All six conformations were optimized independently to find the lowest energy conformation. The structures of transition states were optimized from the guessed structures obtained either by gradually changing the distance of leaving group or by optimizing the fixed geometry with the values for the optimized transition state of similar structure. The optimized structures of transition states were verified as having a single imaginary vibrational frequency and a normal mode consistent with the anticipated reaction coordinate from the calculated frequencies. Transition states also had six possible conformations mostly for a single reaction. Thus, all six conformations were tested for the calculations. All energy was optimized at the HF/3-21G* level and corrected with unscaled zero point energy. All kinetic simulations were performed using Chemical Kinetics Simulator[36] (version 1.01).

(33) Pangborn, A. B.; Giardello, M. A.; Grubbs, R. H.; Rosen, R. K.; Timmers, F. J. *Organometallics* **1996**, *15*, 1518.
(34) Spartan version 5.0, Wavefunction, Inc.: Irvine, CA.
(35) Frisch, M. J.; Trucks, G. W.; Schlegel, H. B.; Scuseria, G. E.; Robb, M. A.; Cheeseman, J. R.; Zakrzewski, V. G.; Montgomery, J. A., Jr.; Stratmann, R. E.; Burant, J. C.; Dapprich, S.; Millam, J. M.; Daniels, A. D.; Kudin, K. N.; Strain, M. C.; Farkas, O.; Tomasi, J.; Barone, V.; Cossi, M.; Cammi, R.; Mennucci, B.; Pomelli, C.; Adamo, C.; Clifford, S.; Ochterski, J.; Petersson, G. A.; Ayala, P. Y.; Cui, Q.; Morokuma, K.; Malick, D. K.; Rabuck, A. D.; Raghavachari, K.; Foresman, J. B.; Cioslowski, J.; Ortiz, J. V.; Stefanov, B. B.; Liu, G.; Liashenko, A.; Piskorz, P.; Komaromi, I.; Gomperts, R.; Martin, R. L.; Fox, D. J.; Keith, T.; Al-Laham, M. A.; Peng, C. Y.; Nanayakkara, A.; Gonzalez, C.; Challacombe, M.; Gill, P. M. W.; Johnson, B.; Chen, W.; Wong, M. W.; Andres, J. L.; Gonzalez, C.; Head-Gordon, M.; Replogle, E. S.; Pople, J. A. *Gaussian 98*, revision A.11; Gaussian, Inc.: Pittsburgh, PA, 1998.
(36) Chemical Kinetics Simulator was obtained from the IBM's Almaden Research Center Web site: http://www.almaden.ibm.com/st/msim/ckspa_n-t.html.

Dimethylsulfoxonium Methylide 1. General Method. To a flame-dried, three-necked flask fitted with a reflux condenser connected to a nitrogen inlet was added a 60% dispersion of NaH (4.05 g, 101 mmol) in mineral oil. The dispersion of NaH in mineral oil was washed with dry hexanes (3 × 30 mL). Trimethylsulfoxonium chloride (9.5 g, 74 mmol) was added to the flask, and anhydrous toluene (90 mL) was added. The reaction mixture was vigorously stirred and heated to 110 °C. The reaction solution was allowed to stir at reflux until the evolution of H_2 ceased and the color of the solution changed from gray to white. The ylide solution in toluene was filtered through a Schlenk filter containing dry Celite 545 under N_2. An aliquot of the ylide solution (0.250 mL) in water was treated with 1 drop of a solution of phenolphthalein in EtOH and titrated with 0.1000 N HCl. The concentration was 0.61 M. The yield was 76%. The ylide solution was stored at −20 °C and remained stable for several weeks.

1-Boraadamantane THF 2. The procedure of Mikhailov and co-workers was followed to synthesize **2**.[11] To a flame-dried, two-neck 50 mL flask with a stir bar and condenser was added 3-methoxy-7-(methoxymethyl)-3-borabicyclo[3.3.1]non-6-ene (2.8698 g, 14.8 mmol). A solution of borane THF (14.80 mL, 1 M, 14.8 mmol) was slowly added with stirring. The reaction was exothermic and came to reflux during addition of the borane THF. The reaction solution was then lowered into an oil bath preheated to 80 °C and refluxed for 1 h. The THF was removed by distillation at atmospheric pressure under nitrogen, followed by vacuum distillation (20 mmHg). The white residue was then sublimed under vacuum (0.100 mmHg, 70 °C) onto an ice-water chilled coldfinger to yield 1-boraadamantane THF **2** (1.6140 g, 53%) as a solid white crystalline compound, mp 89−91 °C. ^{1}H NMR (500 MHz, C_6D_6): δ 3.34 (t, J = 6.8, 4H), 2.74 (br s, 3H), 2.00 (m, 6H), 1.01 (m, 10H). ^{13}C NMR (125.8 MHz, C_6D_6): δ 68.4, 40.7, 34.6, 29.7 (br s), 24.3. ^{11}B NMR (237 MHz, $CDCl_3$): δ 5.10 (br s). IR (KBr): 2868, 1438, 1350, 1299, 1252, 1226, 1192, 1119, 1078, 1025, 982, 930, 918, 855, 728, 614 cm^{-1}. HRMS (CI): *m/z* calcd for $C_{13}H_{24}BO$ $(M + H)^+$ 207.1923, found 207.1929.

Star Polymer 4. General Method. Toluene solutions of ylide **1** were preheated to 80 °C and treated with an aliquot of a toluene solution of 1-boraadamantane•THF (**2**). The ylide was rapidly consumed (5 min), and trimethylamine-*N*-oxide dihydrate (3.1 equiv) was added to effect oxidation under reflux conditions. Removal of solvents followed by filtering and washing of the polymeric solids with methanol, water, and hexanes gave near quantitative crude yields of polymeric triol **4**. Purification by reprecipitation in toluene/acetonitrile afforded a purified white polymer **4** in high yield, mp 125 °C (spectroscopic data for trial 2 of Table 1). ^{1}H NMR (500 MHz, C_6D_6, 78 °C): δ 3.38 ppm (t, J = 6.4 Hz, 6H), 1.85 ppm (d, J = 12.2, 3H), 1.35 (m (br), 890H), 0.94 (d, J = 6.4, 3H), 0.59 ppm (q, J = 11.8, 3H), 0.50 (s, 3H). ^{13}C NMR (125.8 MHz, C_6D_6, 78 °C): δ 62.8, 40.9, 38.2, 38.1, 37.6, 33.3, 30.6, 30.5, 30.1, 30.0, 29.9, 27.6, 27.5, 26.2, 20.0. IR: 3422 (br), 2918, 1473, 1057, 719 cm^{-1}. M_N = 5595 (GPC).

3-Methoxy-7-(methoxymethyl)-3-borabicyclo[3.3.1]non-6-ene 5. The method of Mikhailov and co-workers was followed to synthesize **5**.[11] To a flame-dried, two-neck 50 mL flask with a stir bar and condenser was added distilled triallylborane (**6**) (8.5 g, 63 mmol) under a nitrogen atmosphere. The flask was heated with stirring under nitrogen at 130 °C in a preheated oil bath (10 min). Methyl propargyl ether (4.5 mL, 64 mmol) was added via syringe over the course of 10 min to the stirring triallylborane. The reaction was heated at 130 °C for 1 h. The reaction solution was cooled to room temperature, and methanol (2.9 mL, 72 mmol) was added dropwise under nitrogen with stirring. The reaction was exothermic and accompanied by the evolution of propylene gas. After an additional 5 min of stirring, the reaction mixture was distilled under vacuum (0.10 mmHg) with a short-path distillation head at a head temperature of 79 °C to give NMR-pure 3-methoxy-7-(methoxymethyl)-3-borabicyclo[3.3.1]non-6-ene **5** (10.75 g, 87%) as a clear, viscous liquid. ^{1}H NMR (500 MHz, $CDCl_3$): δ 5.66 (br s, 1H), 3.74 (d, J = 11.7, 1H), 3.64 (d, 11.8), 3.58 (s, 3H), 3.19 (s, 3H), 2.49 (br s, 1H), 2.43 (br s, 1H), 2.25 (d, J = 17.9, 1H), 1.74 (d, J = 12.7, 1H), 1.70 (d, J = 17.8, 1H), 1.60 (d, J = 12.7, 1H), 1.04 (d, J = 17.4, 1H), 0.96 (dd, J = 17, 7.5, 1H), 0.86 (d, J = 17.4, 1H), 0.83 (dd, J = 17, 5.3, 1H). ^{13}C NMR (125.8 MHz, $CDCl_3$): δ 131.7, 130.8, 77.0, 56.9, 53.0, 34.9, 32.5, 29.0, 26.9, 25.4 (br s), 24.1 (br s). ^{11}B NMR (237 MHz, $CDCl_3$): δ 55.4 (br s). IR (thin film): 3397, 2909, 1465, 1431, 1371, 1298, 1167, 1101, 1038, 1019, 996, 955, 914, 880, 847, 831, 678 cm^{-1}. HRMS (EI/hexanes): *m/z* calcd for $C_{11}H_{19}BO_2$ (M^+) 194.1478, found 194.1481.

Triallylborane 6. The protocol of Zhakarkin and co-workers was followed to synthesize **6**.[12] To a flame-dried 250 mL round-bottom flask sealed with rubber septum and equipped with a magnetic stir bar, reflux condenser, and thermometer were transferred solid aluminum granules (12.03 g, 446 mmol) and $HgCl_2$ (s) (88 mg, 0.32 mmol). Dry, N_2 purged diethyl ether (60 mL) was added, and the solution was stirred and heated to 35 °C. Allyl bromide (52.1 mL, 602 mmol) was added dropwise under a nitrogen atmosphere. Care must be taken to add the allyl bromide slowly, because the reaction with aluminum is exothermic. The reaction mixture was stirred at reflux in an oil bath set at 67 °C for 3 h. The reaction mixture was then transferred via syringe into a septum sealed flame-dried 250 mL round-bottom flask containing BF_3•Et_2O (20.0 mL, 142 mmol) under nitrogen. This solution was refluxed at 70 °C for 3 h. The ether was removed by short-path distillation under nitrogen. The residue was then distilled under vacuum (20 mmHg) with a short-path distillation head at a head temperature of 65 °C to give crude triallylborane as a clear, colorless liquid (17.00 g, 78%). ^{11}B NMR (237 MHz, $CDCl_3$) of this distillate showed a major peak, δ 80.7 (br s) 83%, and minor peaks at δ 50.6 (br s) 11%, and δ 32.0 (br s) 6%. The peak at δ 80.7 (br s) has been assigned to triallylborane. On the basis of chemical shift, the peak at δ 50.6 has been tentatively assigned to a borinic ester of some type, most likely the product of the triallylborane's reaction with oxygen. A second vacuum distillation (20 mmHg) yielded pure triallylborane as a clear, colorless liquid (13.07 g, 60%). ^{1}H NMR (500 MHz, $CDCl_3$): δ 2.2 (br s, 6H), 4.9 (br s, 6H), 5.89−5.98 (p, J = 10.6, 3H). ^{13}C NMR (125.8 MHz, $CDCl_3$): δ 134.8, 114.7 (br s), 34.4 (br s). ^{11}B NMR (237 MHz, $CDCl_3$): δ 80.6 (br s). IR (neat): 3076, 2999, 2973, 2914, 1807, 1635, 1420, 1370, 1270, 1170, 993, 900 cm^{-1}.

***cis*-1,3,5-Trihydroxymethylcyclohexane 7.** To a solution of 1-boraadamantane THF **2** (1.47 g, 7.1 mmol) in toluene (18 mL) was added trimethylamine *N*-oxide dihydrate (2.39 g, 21.4 mmol), and the solution was refluxed for 16 h. After the solution cooled to 100 °C, 1 mL of H_2O was added. The toluene, trimethylamine, and H_2O were removed in vacuo, and the residue was purified by flash chromatography (9:1 EtOAc:MeOH) and recrystallized in acetone to give the triol **7** (0.944 g, 76%) as a white crystalline solid, mp 96−98 °C.[9] ^{1}H NMR (500 MHz, D_2O): δ 3.36 (d, J = 6.3, 6H), 1.68 (d, J = 12.5, 3H), 1.52 (m, 3H), 0.50 (q, J = 12.2, 3H). ^{13}C NMR (125.8 MHz, D_2O): δ 31.8, 35.8, 67.3. IR: 3356, 2915, 1064, 1024 cm^{-1}. HRMS (CI): *m/z* calcd for $C_9H_{19}O_3$ $(M + H)^+$ 175.1334, found 175.1338.

1-Borahomoadamantane DMSO 9. To a solution of 1-boraadamantane THF **2** (1.67 g, 8.0 mmol) in toluene (12 mL) at −78 °C was slowly added a solution of dimethylsulfoxonium methylide in toluene (17.0 mL, 0.49 M, 8.3 mmol). The reaction was maintained at −78 °C overnight. The resulting white crystals that precipitated were filtered, washed with hexanes, transferred to a 20 dram vial, and dried under high vacuum (1 mmHg) at −60 °C for 3 h. Upon warming to room temperature under high vacuum (1 mmHg), the white crystals melted to a liquid, releasing heat, and resolidified upon cooling. The white residue was then sublimed under vacuum (0.100 mmHg, 73 °C) onto an ice-water chilled coldfinger to yield 1-borahomoadamantane DMSO **9** (1.18 g, 65%) as a solid white crystalline compound, mp 73−75 °C. ^{1}H NMR (500 MHz, DMSO-d_6): δ 2.52 (s, 6H), 1.90 (m, 2H), 1.86 (m, 1H), 1.70 (m, 2H), 1.48 (m, 2H), 1.26 (m, 4H), 0.50 (m, 6H). ^{13}C NMR (125.8 MHz, DMSO-d_6): 40.4, 39.1, 39.0, 33.0, 32.8, 31.5, 29.2, 23.7. ^{11}B NMR (237 MHz, DMSO-d_6): δ 5.7 (br s). IR (KBr): 2892,

1406, 1033, 912, 846, 635, 565 cm^{-1}. HRMS (CI): *m/z* calcd for $C_{12}H_{24}OBS$ $(M + H)^+$ 227.1643, found 227.1647.

***cis*-1-Hydroxyethyl-3,5-bis(hydroxymethyl)cyclohexane 10.** To a solution of 1-borahomoadamantane·DMSO **9** (0.65 g, 2.9 mmol) in toluene (7.0 mL) was added trimethylamine-*N*-oxide dihydrate (0.97 g, 8.6 mmol), and the reaction was refluxed overnight. The toluene, trimethylamine, and H_2O were removed in vacuo, and the residue was purified by flash chromatography (9:1 $CHCl_3$:MeOH) to give the triol **10** (0.47 g, 87%) as an oil. ^{1}H NMR (500 MHz, D_2O): δ 3.54 (t, J = 6.5, 2H), 3.30 (d, J = 11.8, 4H), 1.64 (d, J = 12.0, 3H), 1.45 (m, 2H), 1.38 (m, 3H), 0.46 (q, J = 12.2, 3H). ^{13}C NMR (125.8 MHz, D_2O): δ 67.6, 59.9, 39.3, 35.9, 33.1, 32.3. IR: 3332, 2914, 1062, 1015 cm^{-1}. HRMS (CI): *m/z* calcd for $C_{10}H_{21}O_3$ $(M + H)^+$ 189.1490, found 189.1493.

***cis*-1,3,5-Tris(hydroxymethyl)cyclohexane Triacetate 11.** To a finely crushed powder of *cis*-1,3,5-trihydroxymethylcyclohexane (**7**) (0.20 g, 1.1 mmol) was added acetic anhydride (5.0 mL, 53.0 mmol) with stirring at room temperature. The reaction solution was heated to 100 °C and stirred (1 h). The reaction was observed to be complete by TLC. The excess acetic anhydride was removed in vacuo, and the crude product was purified by flash chromatography (3:1 hexanes:EtOAc) to give the triacetate **11** (0.29 g, 83%) as a colorless oil. ^{1}H NMR (500 MHz, $CDCl_3$): δ 3.86 (d, J = 6.2, 6H), 1.98 (s, 9H), 1.76 (d, J = 14.4, 3H), 1.69 (m, 3H), 0.65 (q, J = 12.4, 3H). ^{13}C NMR (125.8 MHz, $CDCl_3$): δ 170.5, 68.9, 36.0, 32.4, 21.0. IR (neat): 2942, 1739, 1463, 1369, 1242, 1035 cm^{-1}. HRMS (CI): *m/z* calcd for $C_{15}H_{28}NO_6$ $(M + NH_4)^+$ 318.1916, found 318.1915.

***cis*-1-Hydroxyethyl-3,5-bis(hydroxymethyl)cyclohexane Triacetate 12.** To *cis*-1-hydroxyethyl-3,5-dihydroxymethylcyclohexane (**10**) (0.30 g, 1.6 mmol) was added acetic anhydride (7.1 mL, 75.2 mmol) with stirring. The reaction solution was heated to 100 °C and maintained at this temperature (3 h) with stirring. The reaction was observed to be complete by TLC. The excess acetic anhydride was removed in vacuo, and the crude product was purified by flash chromatography (3:1 hexanes:EtOAc) to give the triacetate **12** (0.44 g, 86%) as a colorless oil. ^{1}H NMR (500 MHz, $CDCl_3$): δ 4.09 (t, J = 6.7, 2H), 3.88 (d, J = 6.3, 4H), 2.04 (s, 6H), 2.02 (s, 3H), 1.77 (d, J = 14.0, 3H), 1.71 (m, 2H), 1.55 (q, J = 6.7, 2H), 1.47 (m, 1H), 0.66 (p, J = 12.7, 3H). ^{13}C NMR (125.8 MHz, $CDCl_3$): δ 171.1 (two peaks), 69.0, 62.3, 36.3, 35.7, 35.69, 33.3, 32.3, 21.0, 20.9. IR (neat): 2922, 1739, 1461, 1366, 1240, 1034 cm^{-1}. Anal. Calcd for $C_{16}H_{26}O_6$: C, 61.13; H, 8.34. Found: C, 60.91; H, 8.34. HRMS (CI): *m/z* calcd for $C_{16}H_{27}O_6$ $(M + H)^+$ 315.8070, found 315.8070.

***cis*-1-Hydroxymethyl-3,5-bis(hydroxyethyl)cyclohexane 13a.** To 1-borahomoadamantane·DMSO (**9**) (0.85 g, 3.8 mmol) dissolved in toluene (9 mL) was added a solution of ylide **1** in toluene (5.9 mL, 0.64 M, 3.8 mmol) at −50 °C. After being warmed to 0 °C with stirring (2 h), the reaction was warmed to room temperature with stirring (2 h). Trimethylamine-*N*-oxide dihydrate (1.29 g, 11.6 mmol) was added, and the reaction was heated to 114 °C with stirring (12 h). Solvents were removed in vacuo, and the residue was purified by column chromatography (SiO_2, $CHCl_3$:EtOH 17:3) to give a mixture of triols **10**, **13a**, and **14a** as a clear, colorless oil (0.73 g, 95%). A sample of the crude product was purified by preparative TLC (SiO_2, $CHCl_3$:EtOH 17:3) to allow the isolation of triol **13a** as a clear, colorless oil (0.010 g). ^{1}H NMR (500 MHz, D_2O): δ 3.49 (t, J = 6.5, 4H), 3.26 (d, J = 6.4, 2H), 1.58 (m, 3H), 1.39 (m, 2H), 1.32 (m, 5H), 0.42 (m, 3H). ^{13}C NMR (125.8 MHz, $CDCl_3$): δ 67.4, 59.7, 39.3, 39.2, 38.9, 35.5, 33.0. IR (neat): 3334 (br), 2913, 1648, 1438, 1377, 1049, 1012 cm^{-1}. HRMS (CI): *m/z* calcd for $C_{11}H_{23}O_3$ $(M + H)^+$ 203.1647, found 203.1645.

***cis*-1-Hydroxymethyl-3,5-bis(hydroxyethyl)cyclohexane Triacetate 13b.** To 1-borahomoadamantane·DMSO (**9**) (0.55 g, 2.4 mmol) dissolved in toluene (7 mL) was added a solution of ylide **1** in toluene (3.8 mL, 0.65 M, 2.5 mmol) at −50 °C. After being warmed to 0 °C with stirring (2 h), the reaction was warmed to room temperature with stirring (2 h). Trimethylamine-*N*-oxide dihydrate (0.84 g, 7.5 mmol) was added, and the reaction was heated to 114 °C with stirring (12 h). Solvents were removed in vacuo, and the residue was purified by column chromatography (SiO_2, $CHCl_3$:EtOH 17:3). To the purified residue was added acetic anhydride (12 mL, 126 mmol), and the reaction was heated to 100 °C with stirring for 1 h. The excess acetic anhydride was removed in vacuo, and the crude product was purified by column chromatography (SiO_2, hexanes:EtOAc 23:2) to give a mixture of triacetates **13b**, **14b**, and **15b** as a clear, pale yellow oil (0.74 g, 93% yield). Triacetate **13b** accounted for 43% of the mixture by GC (0.31 g). A sample of triacetate **13b** was obtained by column chromatography (SiO_2, hexanes:EtOAc 23:2) as a clear, pale yellow oil (0.015 g). ^{1}H NMR (500 MHz, $CDCl_3$): δ 4.12 (t, J = 6.8, 4H), 3.89 (d, J = 6.4, 2H), 2.07 (s, 3H), 2.06 (s, 6H), 1.79 (m, 3H), 1.62 (m, 2H), 1.55 (m, 3H), 1.47 (m, 2H), 0.64 (m, 3H). ^{13}C NMR (125.8 MHz, $CDCl_3$): δ 171.2, 69.2, 62.5, 39.4, 36.7, 35.8, 33.7, 21.0, 20.9. IR (neat): 2922, 1738, 1462, 1367, 1237, 1033, 805 cm^{-1}. HRMS (CI): *m/z* calcd for $C_{17}H_{29}O_6$ $(M + H)^+$ 329.1964, found 329.1964.

***cis*-1-Hydroxymethyl-3-hydroxyethyl-5-hydroxypropylcyclohexane 14a.** To 1-borahomoadamantane·DMSO (**9**) (0.85 g, 3.8 mmol) dissolved in toluene (9 mL) was added a solution of ylide **1** in toluene (5.9 mL, 0.64 M, 3.8 mmol) at −50 °C. After being warmed to 0 °C with stirring (2 h), the reaction was warmed to room temperature with stirring (2 h). Trimethylamine-*N*-oxide dihydrate (1.29 g, 11.6 mmol) was added, and the reaction was heated to 114 °C with stirring (12 h). Solvents were removed in vacuo, and the residue was purified by column chromatography (SiO_2, $CHCl_3$:EtOH 17:3) to give a mixture of triols **10**, **13a**, and **14a** as a clear, colorless oil (0.73 g, 95%). A sample of the crude product was purified by preparative TLC (SiO_2, $CHCl_3$:EtOH 17:3) to allow the isolation of triol **14a** as a clear, colorless oil (0.030 g). ^{1}H NMR (500 MHz, D_2O): δ 3.59 (t, J = 6.6, 2H), 3.51 (t, J = 6.7, 2H), 3.35 (d, J = 6.3, 2H), 1.69 (m, 3H), 1.51 (m, 3H), 1.41 (m, 3H), 1.29 (m, 1H), 1.19 (m, 2H), 0.51 (m, 3H). ^{13}C NMR (125.8 MHz, $CDCl_3$): δ 67.5, 62.2, 59.7, 39.4, 39.3, 39.0, 36.1, 35.6, 35.5, 33.1, 32.9, 28.8. IR (neat): 3359 (br), 2912, 1658, 1455, 1360, 1053, 1012 cm^{-1}. HRMS (CI): *m/z* calcd for $C_{12}H_{25}O_3$ $(M + H)^+$ 217.1804, found 217.1806.

***cis*-1-Hydroxymethyl-3-hydroxyethyl-5-hydroxypropylcyclohexane Triacetate 14b.** To 1-borahomoadamantane·DMSO (**9**) (0.55 g, 2.4 mmol) dissolved in toluene (7 mL) was added a solution of ylide **1** in toluene (3.8 mL, 0.65 M, 2.5 mmol) at −50 °C. After being warmed to 0 °C with stirring (2 h), the reaction was warmed to room temperature with stirring (2 h). Trimethylamine-*N*-oxide dihydrate (0.84 g, 7.5 mmol) was added, and the reaction was heated to 114 °C with stirring (12 h). Solvents were removed in vacuo, and the residue was purified by column chromatography (SiO_2, $CHCl_3$:EtOH 17:3). To the purified residue was added acetic anhydride (12 mL, 126 mmol), and the reaction was heated to 100 °C with stirring for 1 h. The excess acetic anhydride was removed in vacuo, and the crude product was purified by column chromatography (SiO_2, hexanes:EtOAc 23:2) to give a mixture of triacetates **13b**, **14b**, and **15b** as a clear, pale yellow oil (0.74 g, 93% yield). Triacetate **14b** accounted for 31% of the mixture by GC (0.23 g). A sample of triacetate **14b** was obtained by column chromatography (SiO_2, hexanes:EtOAc 23:2) as a clear, pale yellow oil (0.03 g). ^{1}H NMR (500 MHz, $CDCl_3$): δ 4.12 (t, J = 6.8, 2H), 4.05 (t, J = 6.8, 2H), 3.89 (d, J = 6.4, 2H), 2.07 (s, 3H), 2.06 (s, 6H), 1.78 (m, 3H), 1.70 (m, 3H), 1.67 (m, 2H), 1.54 (m, 2H), 1.45 (m, 1H), 1.35 (m, 1H), 1.27 (m, 2H), 0.61 (m, 3H). ^{13}C NMR (125.8 MHz, $CDCl_3$): δ 171.9, 69.4, 64.7, 62.5, 39.5, 36.8, 36.4, 36.0, 35.9, 35.8, 33.8, 33.3, 25.9, 21.1, 21.0, 20.9. IR (neat): 2920, 1739, 1366, 1240, 1034 cm^{-1}. HRMS (CI): *m/z* calcd for $C_{18}H_{31}O_6$ $(M + H)^+$ 343.2120, found 343.2121.

***cis*-1-Hydroxymethyl-3,5-bis(hydroxybutyl)cyclohexane Triacetate 20.** To 1-boraadamantane·THF (**2**) (0.20 g, 1 mmol) dissolved in toluene (10 mL) was added a solution of ylide **1** in toluene (36.0 mL, 0.55 M, 20 mmol) at 25 °C. After the mixture was stirred (2 h), trimethylamine-*N*-oxide dihydrate (0.35 g, 3.1 mmol) was added, and the reaction was heated to 114 °C with stirring (12 h). Solvents were

removed in vacuo, and both the polymeric product (**4**) and the residual triols were purified by column chromatography (SiO_2, $CHCl_3$:EtOH 17:3). To the purified triols was added acetic anhydride (12 mL, 126 mmol), and the reaction was heated to 100 °C with stirring for 1 h. The excess acetic anhydride was removed in vacuo, and the crude product was purified by column chromatography (SiO_2, hexanes:EtOAc 23:2) to give a mixture of triacetates as a clear, pale yellow oil (0.24 g). Triacetate **20** accounted for 35% of the mixture by GC. A sample of triacetate **20** was obtained by column chromatography (SiO_2, hexanes:EtOAc 23:2) as a clear, pale yellow oil (0.005 g). ^{1}H NMR (500 MHz, $CDCl_3$): δ 4.07 (t, J = 6.8, 4H), 3.89 (d, J = 6.4, 2H), 2.09 (s, 3H), 2.07 (s, 6H), 1.75 (m, 3H), 1.65 (m, 3H), 1.36 (m, 12H), 0.57 (m, 3H). ^{13}C NMR (125.8 MHz, $CDCl_3$): δ 171.3, 171.2, 69.6, 64.6, 39.8, 36.9, 36.8, 36.2, 29.7, 28.9, 23.2, 21.0, 20.9. IR (neat): 2924, 1739, 1461, 1366, 1238, 1036 cm^{-1}. HRMS (CI): *m/z* calcd for $C_{17}H_{29}O_6$ $(M + H)^+$ 384.2590, found 384.2600.

Acknowledgment. We thank the Chemistry Division of the National Science Foundation for financial support of this work (Grant CHE-9617475). C.E.W. wishes to thank Allergan, Inc., for a graduate fellowship. Gracious thanks is also given to Dr. A. W. deGroot of the Dow Chemical Co. for analysis of the high molecular weight star polymers.

Supporting Information Available: X-ray data for compounds **2** and **9** (PDF and CIF). This material is available free of charge via the Internet at http://pubs.acs.org.

JA0361291